DispatchDate: 19.10.2021 · ProofNo: 1564, p.1

nature medicine

BRIEF COMMUNICATION

https://doi.org/10.1038/s41591-021-01564-7

Neurocognitive and hypokinetic movement disorder with features of parkinsonism after BCMA-targeting CAR-T cell therapy

Oliver Van Oekelen[1,2,17], Adolfo Aleman[1,2,17], Bhaskar Upadhyaya[2,3,4], Sandra Schnakenberg[5,6], Deepu Madduri[2,3], Somali Gavane[7], Julie Teruya-Feldstein[5], John F. Crary[5,6,8,9,10,11], Mary E. Fowkes[5,6,18], Charles B. Stacy[12], Seunghee Kim-Schulze[3,4,13,14,15], Adeeb Rahman[3,4,13,14], Alessandro Laganà[3,13,16], Joshua D. Brody[2,3,13,14], Miriam Merad[3,4,13,14], Sundar Jagannath[2,3,14] and Samir Parekh[2,3,13,14] ✉

B-cell maturation antigen (BCMA) is a prominent tumor-associated target for chimeric antigen receptor (CAR)-T cell therapy in multiple myeloma (MM). Here we describe the case of a patient with MM who was enrolled in the CARTITUDE-1 trial (NCT03548207) and who developed a progressive movement disorder with features of parkinsonism approximately 3 months after BCMA-targeted ciltacabtagene autoleucel CAR-T cell infusion, associated with CAR-T cell persistence in the blood and cerebrospinal fluid, and basal ganglia lymphocytic infiltration. We show BCMA expression on neurons and astrocytes in the patient's basal ganglia. Public transcriptomic datasets further confirm BCMA RNA expression in the caudate of normal human brains, suggesting that this might be an on-target effect of anti-BCMA therapy. Given reports of three patients with grade 3 or higher parkinsonism on the phase 2 ciltacabtagene autoleucel trial and of grade 3 parkinsonism in the idecabtagene vicleucel package insert, our findings support close neurological monitoring of patients on BCMA-targeted T cell therapies.

MM is a plasma cell disorder that accounts for ~10% of hematologic malignancies[1]. MM is considered incurable and is characterized by multiple relapses of increasingly refractory disease. Immune therapies (including bispecific antibodies and CAR-T cells) have emerged in clinical trials with promising efficacy in MM[2–4]. BCMA (also referred to as TNFRSF17 or CD269) has attracted interest as a tumor-associated target in MM. BCMA is expressed on mature B lymphocytes (for example, plasma cells)[5–7], and its overexpression and activation are associated with MM progression[8]. The ligands for BCMA, APRIL and BAFF are present in the bone marrow and induce differentiation, growth and long-term survival of plasma cells[9,10]. Two BCMA-targeted CAR-T cells have demonstrated efficacy in phase 2 clinical trials in MM, with overall response rates ranging from 73% (idecabtagene vicleucel (ide-cel)) to 97% (ciltacabtagene autoleucel (cilta-cel))[3,11–13].

Cytokine release syndrome (CRS) is a form of systemic inflammatory response syndrome characterized by the elevation of pro-inflammatory cytokines and has been reported in BCMA-targeted CAR-T cell trials. Severity ranges from a mild reaction with flu-like symptoms to a life-threatening cytokine storm and fulminant hemophagocytic lymphohistiocytosis. The exact timing and duration of CRS in BCMA-targeted CAR-T therapy are variable, but most cases present early (within 2 weeks of CAR-T infusion) and are of low-grade severity, manageable with supportive care, steroids, tocilizumab, anakinra and other cytokine inhibitors.

Neurotoxicity has been described in BCMA-targeted CAR-T therapy, typically as transient encephalopathy (immune effector cell-associated neurotoxicity syndrome (ICANS))[14,15]. Reported symptoms include headache, confusion, hallucinations, dysphasia, ataxia, apraxia, tremor and seizures. In a meta-analysis of clinical trials of BCMA-targeted CAR-T, the incidence of neurotoxicity (grade ≥3) was 18%[16]. ICANS usually presents concurrently or shortly after CRS, and management coincides with CRS interventions, including cytokine inhibitors and corticosteroids. Of note, as reported here, the patient displayed delayed neurotoxicity outside the CRS window.

The patient, a 58-year-old male, was diagnosed with smoldering MM in 2004, which progressed to active myeloma in 2015. He presented with relapsed/refractory disease after six previous lines of therapy. The patient was refractory to multiple drugs, including daratumumab, lenalidomide, pomalidomide and carfilzomib, and

[1]Graduate School of Biomedical Sciences, Icahn School of Medicine at Mount Sinai, New York, NY, USA. [2]Department of Medicine, Hematology and Medical Oncology, Icahn School of Medicine at Mount Sinai, New York, NY, USA. [3]Tisch Cancer Institute, Icahn School of Medicine at Mount Sinai, New York, NY, USA. [4]Human Immune Monitoring Center, Icahn School of Medicine at Mount Sinai, New York, NY, USA. [5]Department of Pathology, Molecular and Cell-based Medicine, Icahn School of Medicine at Mount Sinai, New York, NY, USA. [6]Department of Neuroscience, Icahn School of Medicine at Mount Sinai, New York, NY, USA. [7]Department of Diagnostic, Molecular and Interventional Radiology, Icahn School of Medicine at Mount Sinai, New York, NY, USA. [8]Department of Artificial Intelligence and Human Health, Icahn School of Medicine at Mount Sinai, New York, NY, USA. [9]Neuropathology Brain Bank & Research Core, Icahn School of Medicine at Mount Sinai, New York, NY, USA. [10]Ronald M. Loeb Center for Alzheimer's Disease, Icahn School of Medicine at Mount Sinai, New York, NY, USA. [11]Friedman Brain Institute, Icahn School of Medicine at Mount Sinai, New York, NY, USA. [12]Department of Neurology, Icahn School of Medicine at Mount Sinai, New York, NY, USA. [13]Department of Oncological Sciences, Icahn School of Medicine at Mount Sinai, New York, NY, USA. [14]Precision Immunology Institute, Icahn School of Medicine at Mount Sinai, New York, NY, USA. [15]Immunai, New York, NY, USA. [16]Department of Genetics and Genomic Sciences, Icahn School of Medicine at Mount Sinai, New York, NY, USA. [17]These authors contributed equally: Oliver Van Oekelen, Adolfo Aleman. [18]Deceased: Mary E. Fowkes ✉e-mail: samir.parekh@mssm.edu

was a candidate for BCMA-targeted CAR-T therapy. The patient underwent a bridging chemotherapy regimen (melphalan 56.25 mg once and two doses of bortezomib 1.3 mg m^{-2}). Before CAR-T infusion, he received 300 mg m^{-2} of fludarabine and 30 mg m^{-2} of cyclophosphamide daily for 3 d to induce lymphodepletion. The baseline tumor burden was low (3% plasma cells on bone marrow biopsy), but he had multiple extramedullary plasmacytomas.

After cilta-cel infusion (day 1), the patient developed fever on day 9 and hypotension on day 11 (CRS up to maximum grade 3) with the peak of C-reactive protein, ferritin and inflammatory cytokines (TNF-α, IFN-γ, IL-6 and IL-18) 2 weeks after CAR-T infusion. CRS symptoms resolved by day 14 after treatment with tocilizumab and anakinra[17]. Relevant clinical and biochemical parameters, timing of selected therapeutic agents and additional cytokine profiling are shown in Extended Data Figs. 1 and 2. The patient remained afebrile until hospitalization on day 51 with neutropenic fever and pneumonia, treated with empiric antibiotics. Cultures remained negative, but polymerase chain reaction (PCR) detected rhinovirus in respiratory secretions. The patient was discharged at day 57. Disease evaluation (day 79) showed a very good partial response, according to International Myeloma Working Group criteria.

At day 101 after CAR-T cell infusion, the patient was evaluated with complaints of increasing fatigue interfering with daily activities. Initially, we observed slow gait and psychomotor retardation. Subsequent evaluation by two independent neurologists confirmed a clinical syndrome with features of parkinsonism, including bradykinesia, postural instability, hypophonia, hypomimia, micrographia and a mild right-sided (action and resting) tremor, as well as saccadic intrusions on smooth pursuit and impaired short-term memory. There was no cogwheeling, no focal paresis or atrophy, no pathological reflexes or alterations of deep tendon reflexes and no ataxia, and the Romberg test was negative. Sensation was intact. The features were progressive over time with development of increasing hypomimia, rigidity and difficulty initiating movements. There were no recent drug changes or toxin exposure to account for the observed clinical phenotype. The patient was on a benzodiazepine for anxiety disorder, which was discontinued without improvement of the clinical features. Laboratory tests showed fluctuating neutrophil counts due to regular granulocyte–macrophage colony-stimulating factor (GM-CSF) injections (Extended Data Fig. 1c). Magnetic resonace imaging (MRI) of the brain with and without contrast showed only small pre-existing foci of T2/FLAIR signal hyperintensity scattered throughout the periventricular and subcortical white matter (Extended Data Fig. 3a), and lumbar puncture findings were non-explanatory (Supplementary Table 1; additional clinical background is provided in the Methods). A treatment attempt with levodopa because of progressive movement disorder and functional decline was unsuccessful. Fluorodeoxyglucose-positron emission tomography (FDG-PET) of the brain for response evaluation indicated a decreased uptake in the caudate nucleus bilaterally in comparison with imaging of 2 months prior, without any structural abnormalities (Extended Data Fig. 4). Ioflupane (123-I) scan was negative, suggesting a disease mechanism different than Parkinson's disease (Extended Data Fig. 3b).

As shown in Fig. 1a, CAR-T cells were detectable in the blood in large numbers, starting at day 11 after infusion up to day 156. Notably, 70–90% of all T cells in the peripheral blood were CAR-T cells (Fig. 1b). This observation suggested a role for persistent CAR-T cells in the development of the patient's neurologic complaints. Extensive phenotyping of T cells using a mass cytometry (CyTOF) approach (Fig. 1c) suggested that most CAR-T cells had an effector memory phenotype (that is, $CD45RA^{-}CCR7^{-}$) (Fig. 1d and Extended Data Fig. 5). Functional assays of peripheral blood CAR-T cells, isolated 128 d after treatment, confirmed their ability to produce inflammatory cytokines (IFN-γ, TNF-α and GM-CSF) upon PMA/ionomycin stimulation in vitro (Extended Data Fig. 6), highlighting their cytotoxic/pro-inflammatory potential. The full list of cytokines tested and comparison with a healthy donor are shown in Extended Data Fig. 6b. The patient's CAR-T cells did not exhibit a Th17 phenotype—a T cell subtype previously associated with immunologic neurodegenerative disorders. Comparative single-cell analysis of CAR-T cells of this patient with three other patients from the same trial (without parkinsonism) by cellular indexing of transcriptomes and epitopes by sequencing (CITE-seq) (Fig. 1e and Extended Data Fig. 7) showed qualitative transcriptomic differences with significantly higher expression of genes associated with long-term survival (for example, *IL7R*) and genes encoding inflammatory cytokines (*IFNG*, *TNF* and *CSF2*) and lower expression of anti-inflammatory cytokine genes (for example, *IL10*).

Microarray data of healthy human brains of the Allen Brain Atlas[18] confirmed localized RNA expression of BCMA in the basal ganglia and, more specifically, in the caudate nucleus in five of six available specimens (Fig. 2b and Extended Data Fig. 8). We hypothesized that the symptoms could result from CAR-T cell infiltration in the brain targeting BCMA-expressing cells, thereby causing a movement disorder with features of parkinsonism. Analysis of the cerebrospinal fluid (CSF) by fluorescence-activated cell sorting (FACS) confirmed the presence of CAR-T cells in the CSF (0.477 CAR-T cells per µl; Extended Data Fig. 9b). Cytokine profiling of CSF and blood plasma of the patient and a healthy control showed overexpression of multiple cytokines in the patient's CSF associated with T cell chemotaxis (for example, CXCL5, CXCL10 and CXCL11), T cell activation (for example, granzymes, IFN-γ and CD40-L) and blood–brain barrier dysfunction (for example, PDGFb and angiopoetin-1) (Extended Data Fig. 9).

Due to the sustained proliferation of CAR-T cells with spread beyond the blood–brain barrier and progressive decline in the patient's general condition, IV cyclophosphamide (300 mg m^{-2}), IT cytarabine (100 mg) and hydrocortisone (50 mg) were given on day 149, after careful consideration, aiming to rapidly reduce circulating CAR-T cells. We observed a decline of the absolute T cell count in the CSF with a stable fraction of CAR-T cells (0.128 CAR-T cells per

Fig. 1 | Persistence of CAR-T cells with an activated effector memory phenotype in the peripheral blood. a, CyTOF plots gated on $CD3^{+}$ T cells, showing fraction of FITC-BCMA-labeled (that is, CAR) T cells at different time points after CAR-T infusion. **b**, Quantitative representation of data in **a**, showing the relative contribution of $CD4^{+}$ and $CD8^{+}$ CAR-T cells at different time points. The time periods associated with CRS, neutropenic fever and neurotoxicity are annotated. Each bar corresponds to $n=1$ sample collected from the patient. **c**, Schematic illustration of CyTOF strategy used to detect the CAR on the T cell surface (see Methods for details (figure panel created with BioRender)). **d**, CAR-T cell phenotype, as determined by expression of CCR7 and CD45RA, showing a high fraction of effector memory T cells. Each bar corresponds to $n=1$ sample collected from the patient. **e**, *t*-SNE plot representation of CITE-seq analysis of PBMCs before and after PMA/ionomycin stimulation. Clustering was determined by SNF and Louvain clustering algorithm. Individual cells are colored by subject (healthy donor (HD), neurotoxicity patient (NEUROTOX) and three other patients on the same clinical trial without neurotoxicity (MM1, MM2 and MM3)). Highlighted on side plots is expression level of CD4, CD8 and CAR ADT (ADT, representation of protein level, high = red, low = blue) and box plots (median, Q1 and Q3 quartiles and whiskers up to 1.5× interquartile range), showing expression of a subset of differentially expressed genes ($^{*}P<0.01$; NS, $P\geq0.05$; two-sided Mann–Whitney *U*-test) in the patient with neurotoxicity (NEUROTOX, $n=1$, data on 145 stimulated $CD4^{+}$ CAR-T cells (top, red) and 119 stimulated $CD8^{+}$ CAR-T cells (bottom, red) total) and the other MM patients (MM1–3, $n=3$, data on 152 stimulated $CD4^{+}$ CAR-T cells (top, gray) and 406 stimulated $CD8^{+}$ CAR-T cells (bottom, gray) total).

μl; Extended Data Fig. 9c). A second dose of IV cyclophosphamide (300 mg m^{-2}) and IT cytarabine/hydrocortisone were administered on day 156. The patient subsequently developed neutropenic fever with acute respiratory distress syndrome and multi-organ failure and died on day 162.

Postmortem analysis of the caudate nucleus revealed the presence of focal gliosis as shown on hematoxylin and eosin (H&E) staining and immunohistochemistry of glial fibrillary acidic protein (GFAP) (Fig. 2c,d). Immunohistochemistry further showed a T cell infiltrate ($CD3^+$, predominantly $CD8^+$) in the periventricular

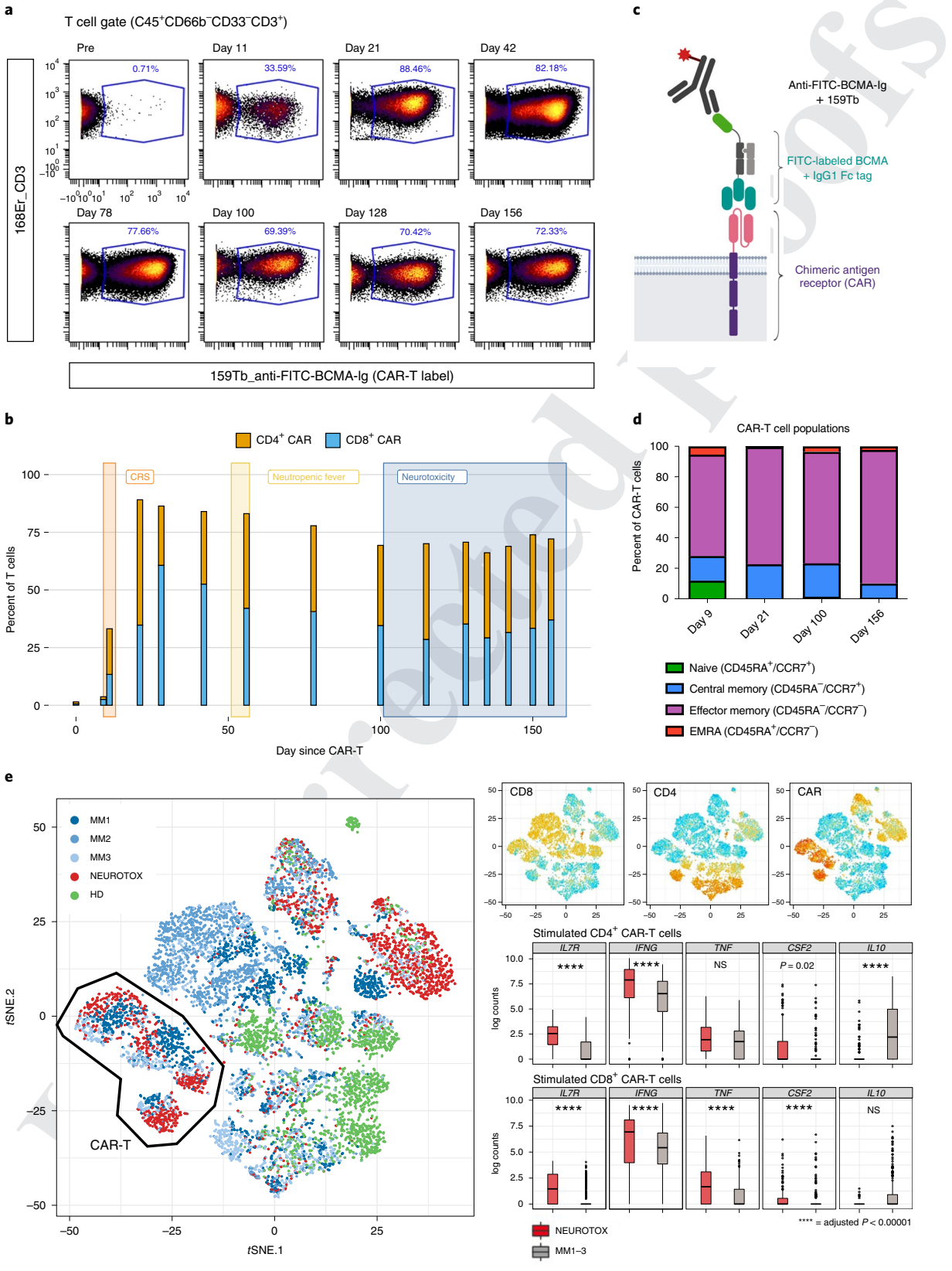

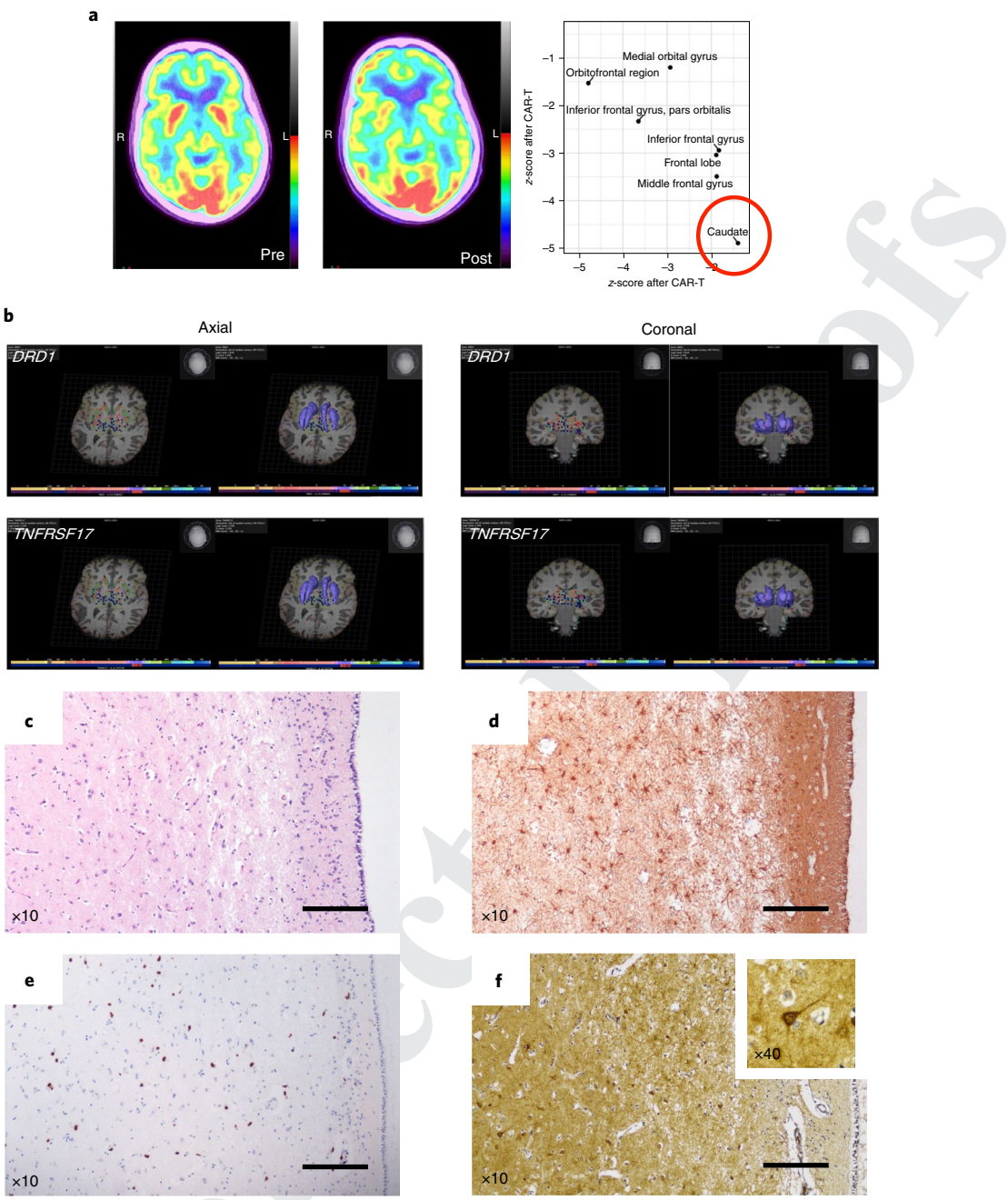

Fig. 2 | BCMA is expressed in the caudate nucleus of healthy donors and postmortem in the patient after CAR-T cell therapy. a, FDG-PET/CT shows decreased uptake in the caudate nucleus after development of neurotoxicity (POST, right, day 134 after CAR-T infusion), compared to previous imaging before development of neurotoxicity symptoms (PRE, left, day 77 after CAR-T infusion). Prior FDG-PET/CT imaging (before CAR-T infusion) was similar to the pre-neurotoxicity scan. The scatter plot on the right illustrates the normalized *z*-score of different regions of the brain before and after CAR-T infusion. The caudate is highlighted. The normalized score is calculated using MIMneuro, comparing the image with a library of 43 FDG neurologic controls (41–80 years old). **b**, Visual representation of the expression of *DRD1* and *TNFRSF17* (BCMA) in a single patient from the Allen Brain Atlas. Expression of both genes (left, red = high) overlaps with the caudate nucleus region shown in three dimensions (right, purple). Image credit: Allen Institute for Brain Science (2010). **c**, H&E staining of the caudate nucleus subependymal region (×10 magnification; scale bar, 200 µm). **d**, GFAP immunohistochemistry of the caudate nucleus subependymal region (×10 magnification; scale bar, 200 µm). **e**, CD3 immunohistochemistry of the caudate nucleus subependymal region (×10 magnification; scale bar, 200 µm). **f**, BCMA immunohistochemistry of the caudate nucleus subependymal region (×10 magnification; scale bar, 200 µm; inset, ×40 magnification showing a neuron staining positively). **c**–**f**, Images shown are representative slides from the caudate nucleus from the patient described in this case report ($n=1$). For each stain, at least three slides were available showing similar results.

region of the basal ganglia (Fig. 2e). BCMA staining was performed (Methods), and we found BCMA expression on a subset of neurons and astrocytes in the caudate nucleus as well as on a layer of neurons in the adjacent frontal cortex (Fig. 2f and Extended Data Fig. 10).

The value of BCMA as a tumor-associated target in MM depends on the selective expression on (malignant) plasma cells. Even though BCMA expression has been extensively characterized on hematopoietic lineages, studies on other tissues are limited[6,7,19]. We found that

microarray data from the Allen Brain Atlas shows BCMA mRNA expression in the basal ganglia and confirmed this in the patient and in a healthy brain (Extended Data Fig. 10) by immunohistochemistry. Assessment of BCMA protein expression on a human tissue array was positive on lymph node, spleen, lung and stomach due to plasma cells present in the bronchus- and mucosa-associated lymphoid tissue, respectively[5]. This tissue array, however, showed some positivity on climbing fibers in the cerebellum and explicitly does not rule out low-density expression in the central nervous system. We acknowledge that these data are, to some extent, conflicting due to lack of standardized protocols for staining tissues, other than bone marrow. A comprehensive evaluation of brain tissue for BCMA protein expression might be warranted to characterize the prevalence and extent of BCMA expression in the central nervous system and confirm the findings of this case report.

BCMA expression on neurologic tissues in a subset of patients could affect the applicability of BCMA-targeted adoptive cell transfer in MM. Implications for other BCMA-targeted immunotherapies—for example, antibody–drug conjugates and bispecific antibodies—are unknown. Even though therapeutic antibodies are thought not to cross the blood–brain barrier, their permeability into the CSF should be carefully evaluated. Other tumor-associated targets are being currently studied in MM, including bispecific antibodies and CAR constructs targeting GPRC5D, FcRH5, CD19, CD38, CD56, CD138 and SLAMF7, some of which have a broader expression outside of plasma cells and warrant careful monitoring[20].

Using chemotherapy to destroy CAR-T cells after infusion is itself associated with toxicity, as this case shows, because the patient died of infectious complications. Other strategies include a modification of CAR structure with engineered suicide genes, the incorporation of inhibitory CAR constructs or usage of a small molecule system as a safety switch to selectively deactivate the CAR-T cells. Recently, CAR natural killer cells have been proposed as an alternative with off-the-shelf use as a potential advantage[20].

This case shows the potential of BCMA-targeted CAR-T cells to cross the blood–brain barrier in a subset of patients and cause a progressive neurocognitive and movement disorder, possibly through targeting of BCMA-expressing cells of the basal ganglia. Neurotoxicity in general has been observed in 23 of 128 patients on ide-cel[11] and in 20 of 97 patients on cilta-cel[13]. Non-ICANS neurotoxicity was not addressed specifically in the ide-cel study but was reported in 12 of 97 patients from the phase 2 study of cilta-cel, of which five patients had a cluster of movement and neurocognitive adverse events (three with grade 3 or higher parkinsonism)[13]. The development of this toxicity in the cilta-cel trial was associated with the presence of two or more risk factors (including high tumor burden, previous grade ≥2 CRS, previous ICANS and high CAR-T cell expansion and persistence). The ide-cel package insert also mentions that grade 3 parkinsonism has occurred after treatment, suggesting that this complication is not necessarily specific to one BCMA-targeted CAR-T cell product. We acknowledge that important questions remain unanswered. Our patient developed neutropenic fever at day 51; it is not well studied whether infections after CAR-T infusion might activate CAR-T cells in vulnerable patients and whether more stringent prophylaxis of infection is warranted. Additional studies to confirm the proposed mechanism of neurotoxicity could help delineate the fraction of patients at risk. In conclusion, our findings suggest that anti-BCMA CAR-T cell therapies, although effective in MM, warrant close monitoring for neurotoxicity, especially as such treatments acquire more widespread implementation in patients with MM.

Online content

Any methods, additional references, Nature Research reporting summaries, source data, extended data, supplementary information, acknowledgements, peer review information; details of author contributions and competing interests; and statements of data and code availability are available at https://doi.org/10.1038/s41591-021-01564-7.

Received: 6 May 2021; Accepted: 28 September 2021;

References

1. Kumar, S. K. et al. Multiple myeloma. *Nat. Rev. Dis. Prim.* **3**, 17046 (2017).
2. Madduri, D., Dhodapkar, M. V., Lonial, S., Jagannath, S. & Cho, H. J. SOHO state of the art updates and next questions: T-cell-directed immune therapies for multiple myeloma: chimeric antigen receptor-modified T cells and bispecific T-cell-engaging agents. *Clin. Lymphoma Myeloma Leuk.* **19**, 537–544 (2019).
3. Shah, N., Chari, A., Scott, E., Mezzi, K. & Usmani, S. Z. B-cell maturation antigen (BCMA) in multiple myeloma: rationale for targeting and current therapeutic approaches. *Leukemia* 34, 985–1005 (2020).
4. Shah, U. A. & Mailankody, S. Emerging immunotherapies in multiple myeloma. *Brit. Med. J.* **370**, m3176 (2020).
5. Bu, D. X. et al. Pre-clinical validation of B cell maturation antigen (BCMA) as a target for T cell immunotherapy of multiple myeloma. *Oncotarget* **9**, 25764–25780 (2018).
6. Carpenter, R. O. et al. B-cell maturation antigen is a promising target for adoptive T-cell therapy of multiple myeloma. *Clin. Cancer Res.* **19**, 2048–2060 (2013).
7. Khattar, P. et al. B-cell maturation antigen is exclusively expressed in a wide range of B-cell and plasma cell neoplasm and in a potential therapeutic target for BCMA directed therapies. *Blood* **130**, 2755–2755 (2017).
8. Sanchez, E. et al. Serum B-cell maturation antigen is elevated in multiple myeloma and correlates with disease status and survival. *Br. J. Haematol.* **158**, 727–738 (2012).
9. Sanchez, E. et al. Soluble B-cell maturation antigen mediates tumor-induced immune deficiency in multiple myeloma. *Clin. Cancer Res.* **22**, 3383–3397 (2016).
10. Tai, Y. T. et al. APRIL and BCMA promote human multiple myeloma growth and immunosuppression in the bone marrow microenvironment. *Blood* **127**, 3225–3236 (2016).
11. Munshi, N. C. et al. Idecabtagene vicleucel in relapsed and refractory multiple myeloma. *N. Engl. J. Med.* **384**, 705–716 (2021).
12. Raje, N. et al. Anti-BCMA CAR T-cell therapy bb2121 in relapsed or refractory multiple myeloma. *N. Engl. J. Med.* **380**, 1726–1737 (2019).
13. Berdeja, J. G. et al. Ciltacabtagene autoleucel, a B-cell maturation antigen-directed chimeric antigen receptor T-cell therapy in patients with relapsed or refractory multiple myeloma (CARTITUDE-1): a phase 1b/2 open-label study. *Lancet* **398**, 314–324 (2021).
14. Lee, D. W. et al. ASTCT consensus grading for cytokine release syndrome and neurologic toxicity associated with immune effector cells. *Biol. Blood Marrow Transpl.* **25**, 625–638 (2019).
15. Neelapu, S. S. et al. Chimeric antigen receptor T-cell therapy—assessment and management of toxicities. *Nat. Rev. Clin. Oncol.* **15**, 47–62 (2018).
16. Gagelmann, N., Ayuk, F., Atanackovic, D. & Kroger, N. B cell maturation antigen-specific chimeric antigen receptor T cells for relapsed or refractory multiple myeloma: a meta-analysis. *Eur. J. Haematol.* **104**, 318–327 (2020).
17. Jatiani, S. S. et al. Myeloma CAR-T CRS management with IL-1R antagonist anakinra. *Clin. Lymphoma Myeloma Leuk.* **20**, 632–636 (2020).
18. Hawrylycz, M. J. et al. An anatomically comprehensive atlas of the adult human brain transcriptome. *Nature* **489**, 391–399 (2012).
19. Lee, L. et al. Evaluation of B cell maturation antigen as a target for antibody drug conjugate mediated cytotoxicity in multiple myeloma. *Br. J. Haematol.* **174**, 911–922 (2016).
20. Shah, U. A. & Mailankody, S. CAR T and CAR NK cells in multiple myeloma: expanding the targets. *Best Pract. Res. Clin. Haematol.* **33**, 101141 (2020).

Methods

Trial design. The CARTITUDE-1 trial (https://clinicaltrials.gov/ct2/show/NCT03548207) is an open-label, single-arm, phase 1b/2 trial that evaluates the safety and efficacy of JNJ-68284528 (cilta-cel), a CAR-T cell therapy directed against BCMA in patients with relapsed or refractory MM. Here we provide the case report of a patient with neurotoxicity enrolled on the CARTITUDE-1 trial. Analysis and reporting follow the CARE guidelines. The CITE-seq experiment includes data on three additional patients with MM who were enrolled on the CARTITUDE-1 trial (a 61-year-old female, a 67-year-old male and a 67-year-old female). Furthermore, all patients with MM included in this work consented to participation in the Multiple Myeloma Biorepository (HSM:18-00456). All patients provided written informed consent for the evaluations. All study protocols were approved by the Program for the Protection of Human Subjects and the Institutional Review Board at the Icahn School of Medicine at Mount Sinai and adhere to the 2008 Declaration of Helsinki.

Sample collection and tissue processing. Peripheral blood was collected in heparin anti-coagulated green tops (10 ml) via venipuncture throughout the course of his treatment in accordance with standard-of-care lab draws. Plasma was isolated from peripheral blood. Peripheral blood mononuclear cells (PBMCs) were Ficoll density separated and cryopreserved. Cryopreserved PBMC samples were used for flow cytometry, mass cytometry and other assays as detailed below. CSF was collected by lumbar puncture in accordance with standard of care. Each sample of 8 ml was centrifuged at 300*g* at 4 °C for 10 min. Then, 0.5 ml of supernatant was divided into aliquots and frozen at −80 °C. Approximately 200 µl of CSF and plasma from peripheral blood were used for Olink and Ella proteomics analysis as detailed below. Cells from CSF were used immediately for flow cytometry.

Statistics and reproducibility. Experiments were not randomized. The investigators were not blinded to allocation during experiments and outcome assessment. No statistical method was used to predetermine sample size for the analyses. For clinical and cytokine assays, no data points were removed from the analysis. Cytometry data were gated to relevant populations, as shown in Extended Data Fig. 5a. CITE-seq data were filtered to remove multiplets based on the crossSampleDoublets() and withinSampleDoublets() functions of the CiteFuse package (version 1.2.0) in R (version 3.6.1). No other cells were excluded from the analysis. The non-parametric Mann–Whitney *U*-test was used to compare gene expression values where appropriate. The Pearson correlation coefficient was used to characterize correlation of cytokine expression between blood and CSF. For all analyses, a two-sided *P* value of less than 0.05 was considered significant.

Additional clinical information on the patient. There was no documented family history of movement disorders for the patient of the case report. In terms of neuro-psychiatric history, the patient had a remote history of migraines, documented in 2009, for which he received sumatriptan 100 mg as needed. In 2014, the patient was diagnosed with a mood disorder and started on sertraline 150 mg. He had been taking lorazepam and alprazolam; these were discontinued at that time, and clonazepam 1 mg daily was started instead. No anti-dopaminergic medications were taken by the patient around this episode or later. Due to recurring anxiety with panic attacks, the sertraline dose was increased to 200 mg, and clonazepam was gradually increased to a maximum daily dose of 4 mg as needed. Sertraline was discontinued in 2016. The clonazepam dose was maintained for recurring anxiety with panic attacks. In addition, the patient was seen at an outside hospital in 2018 after a traffic accident. All documented neurological examinations at that time were normal. He received an MRI of the brain, which noted non-specific punctate foci T2/FLAIR hyperintensity in the periventricular and subcortical white matter, likely secondary to chronic microvascular ischemic disease, but no other intracranial abnormalities. Six months before the CAR-T trial, the patient was seen by a neurologist for the evaluation of weakness in the right hand. The neurological examination and tests of motor function in the limbs were normal, with the exception of portions of the right arm. Symptoms were thought to be suggestive of a radial nerve irritation at the spiral groove related to a work-related overuse problem. Electromyography confirmed mild acute denervation showing a radial nerve injury with mild acute axonal involvement, and the patient's symptoms resolved with rest. During the screening visit for the CAR-T trial, the patient reported grade 1 fatigue, a remote syncope (around 2011) as well as grade 1 peripheral sensory neuropathy (which affects the soles of the feet, toes, calves and fingers), described as cramping without numbness. The neuropathy complaints did not interfere with walking, balance or fine motor movements and developed after bortezomib treatment. During the hospitalization at the time of CAR-T cell infusion, which includes the CRS period, the patient received a neurological evaluation every day. The patient was specifically monitored for neurotoxicity according to the specifications of the clinical trial protocol. Neurological examination was documented at every subsequent study visit (every 28 d) after CAR-T infusion. Additionally, handwriting logs for dexterity were performed as specified. In conclusion, the patient was evaluated by a neurologist 6 months before CAR-T therapy (by the same physician who evaluated the patient when he presented with the described neurotoxicity after CAR-T). He received other neurological examinations immediately before and after CAR-T cell infusion according to the clinical trial protocol. No pre-existing signs of parkinsonism were present during evaluation before CAR-T infusion.

Flow cytometry. Cryopreserved Ficoll density separated PBMCs were thawed by standard technique. Cells in the CSF were used within 3 h of collection after isolation. $CD3^+/CD4^+/CD8^+$ T cell, $CD19^+$ B cell and anti-BCMA-directed T cells were measured by multiple-color flow cytometry with human monoclonal ACROBiosystems anti-BCMA (FITC) (cat. no. BCA-HF254-25µg) and BioLegend human monoclonal anti-CD3 (cat. no. 300472 and cat. no. 344842), human monoclonal anti-CD4 (cat. no. 317434), human monoclonal anti-CD8 (cat. no. 344742) and human monoclonal anti-CD19 (cat. no. 561121). All cell surface antibodies were used at a 1:20 dilution following the manufacturer's recommendations. The FITC-labeled human BCMA was used at a 1:100 dilution. The samples were acquired on a FACS LSRFortessa flow cytometry system (BD Biosciences). Data were visualized and analyzed using Cytobank[21].

Olink multiplex proteomics assay. Relative protein expression was measured in the CSF and peripheral blood plasma using Olink proximity extension technology, a high-throughput multiplex proteomic immunoassay, following the manufacturer's protocols. The commercially available Immuno_Oncology (article no. 95310), which includes 92 immune- and oncology-related, proteins was used. A table with all cytokines measured is included below as Supplementary Table 2. Olink uses marker-specific binding and hybridization of a set of paired oligonucleotide antibody probes that is subsequently amplified using a quantitative PCR. Protein expression values are reported as normalized protein expression values on a $\log_2$ scale. Analysis was conducted in R (version 3.6.1), and figures were produced using the package pheatmap[22].

Ella cytokine detection. The protein simple Ella cytokine detection system uses microfluidics ELISA assays in a multi-analyte chip that were run within cartridges in triplicate following the manufacturer's instructions. Human analytes of IL-6, IL-8, TNF-α, IL18, IFN-γ and IL-10 were performed by the Mount Sinai Human Immune Monitoring Center using 25–30 µl of plasma or CSF from the patient. Analysis was conducted in R, and figures were generated using the package ggplot2 (ref. [23]).

Mass cytometry. Cells were stained with either CyTOF antibody Panel 1 or CyTOF antibody Panel 2 listed in Supplementary Tables 3 and 4. Antibodies used were either purchased pre-conjugated with metals from Fluidigm or purchased unconjugated and metal conjugated in-house at the Human Immune Monitoring Center, Icahn School of Medicine. All in-house conjugated antibodies were titered and validated on healthy donor PBMCs. All antibodies for CyTOF listed in Supplementary Tables 3 and 4 were used at a dilution of 1:100. For longitudinal monitoring of phenotypic changes, cells from selected time points were thawed and labeled with Rh103 intercalator (Fluidigm) as a viability dye and cell proliferation marker IdU (Cell-ID 127 5-Iodo-2′-deoxyuridine, Fluidigm). Cells were initially stained with a cocktail of surface antibodies that included BCMA-FITC (ACROBiosystems) (Panel 1). Surface-stained cells were further stained with polyclonal anti-FITC-159Tb (source) and fixed with 1.6% formaldehyde. Each time point was then barcoded with CyTOF Cell-ID 20-Plex Palladium Barcoding Kit (Fluidigm). Barcoded cells were fixed and permeabilized with Fix-Perm buffer (BD Biosciences) and stained with the remaining intracellular antibodies from CyTOF Panel 1. Intracellular cytokine expression was monitored using CyTOF Panel 2. Cells from selected time points were activated with PMA/ionomycin (BioLegend) in the presence of brefeldin-A (BioLegend) for 6 h. After activation, cells were stained with Rh103 intercalator and stained with BCMA-FITC and fixed with 1.6% formaldehyde. Fixed cells were palladium barcoded with CyTOF Cell-ID 20-Plex Palladium Barcoding Kit and pooled and stained with surface markers from CyTOF Panel 2, including polyclonal anti-FITC-169Tm. Cells stained with surface antibodies were fixed and permeabilized with Fix-Perm buffer and stained with cytokine antibodies. Samples stained with either CyTOF antibody Panel 1 or CyTOF antibodyPanel 2 were finally fixed in freshly diluted 2.4% formaldehyde containing 125 nM intercalator-Ir (Fluidgm) and 300 nM OsO_4 (Acros Organics) and stored at 4 °C in cell staining buffer containing (Fluidigm) 125 nM intercalator-Ir until acquisition. Samples for CyTOF acquisition were washed with CAS buffer (Fluidigm) and re-suspended in CAS buffer containing EQ normalization beads (Fluidigm) and acquired on CyTOF2 (Fluidigm). After acquisition, the data were normalized using the bead-based normalization algorithm in the CyTOF software (Fluidigm). Normalized data were de-barcoded using methods and software developed by Gary Nolan's group at Stanford University School of Medicine[24]. Normalized and de-barcoded data were uploaded to Cytobank[21] for final analysis, as detailed below.

Mass cytometry data analysis. Data in FCS file format were downloaded from Cytobank[21]. For analysis of mass cytometry data, we used a workflow based on the example by Nowicka et al.[25] using the diffcyt[26] and CATALYST[27] packages in R (version 3.6.1). In brief, data were imported and transformed for analysis using the read.flowSet() function from the flowCore package[28] and the prepData(…,

cofactor = 5) function from the CATALYST package, respectively. Clustering was based on the FlowSOM algorithm[29] using all protein markers from the panel on a 10 × 10 grid size with a maximum of $K = 20$ clusters. These clusters were visualized using uniform manifold approximation and projection dimension reduction and subsequently annotated based on canonical protein markers and the FITC-BCMA tag to identify CAR-T cells.

CITE-seq. For each sample, cell suspensions were split and barcoded using 'hashing antibodies' staining β-2-microglobulin and CD298 and conjugated to 'hash-tag' oligonucleotides (HTOs). Before hashing, each of the five samples was split into two aliquots and either 'stimulated' or 'unstimulated'. Stimulated aliquots were incubated for 3 h at 37 °C with PMA/ionomycin. Unstimulated aliquots were incubated for 3 h at 37 °C with cRPMI. After these incubations, the ten aliquots were hashed and pooled. Hashed samples were pooled and stained with CITE-seq antibodies purchased from the BioLegend TotalSeq catalog; the FITC antibody was a custom conjugate from BioLegend. All commercial antibodies were diluted at 1:100 according to the manufacturer's instructions. The custom conjugate is titered to find the optimal volume to stain PBMCs. The CITE-seq panel is detailed in Supplementary Table 5. Stained cells were then encapsulated for single-cell reverse transcription using the 10x Chromium platform (5′, version 1.0), and libraries were prepared according to the manufacturer's instructions with minor modifications summarized hereafter. In brief, cDNA amplification was performed in the presence of 2pM of an antibody oligo-specific primer to increase yield of antibody-derived tags (ADTs) and 3pM of specific primer to increase the yield of HTOs. The amplified cDNA was then separated by SPRI size selection into cDNA fractions containing mRNA-derived cDNA (>300 bp) and ADT-derived cDNA (<180 bp), which were further purified by additional rounds of SPRI selection. Independent sequencing libraries were generated from the mRNA and ADT cDNA fractions, which were quantified, pooled and sequenced together on an Illumina NextSeq/NovaSeq to a targeted depth of 25–750 million reads per gene expression library and 1,000–30,000 targeted reads per cell.

CITE-seq data analysis. Illumina sequencer base call files were de-multiplexed into FASTQ files using the cellranger (version 3.0.1) mkfastq and count pipeline. CITE-seq data were analyzed using R (version 3.6.1) and the CiteFuse package[30], using the proposed analysis pipeline with minor modifications. In brief, matrices with counts representing RNA, ADT and HTO data, respectively, were read into R separately and combined into a SingleCellExperiment object[31] using the preprocessing() function. Metadata (including patient ID and experimental condition (stimulated versus unstimulated)) were added based on known experimental design and corresponding HTOs. HTO expression was normalized using the log-transform method and the normaliseExprs() function. Cross-sample doublets and within-sample doublets were identified and removed using the crossSampleDoublets() and withinSampleDoublets(…, minPts = 10) functions, respectively. Similarity network fusion (SNF) was used to integrate RNA and ADT matrices after calculating log-transformed normalized expression values with the CiteFuse() function. Both spectral clustering with $K = 25$ and Louvain clustering were attempted, and *t*-distributed stochastic neighbor embedding (*t*-SNE) was used to visualize dimension reduction. Manual inspection and canonical gene and protein expression were used to identify clusters corresponding to $CD4^+$ and $CD8^+$ CAR-T cells. These cells were isolated into distinct SingleCellExperiment objects for downstream analysis. SNF, clustering and dimension reduction of CAR-T cells was done in a similar fashion as detailed above. The DEgenesCross() function with standard parameters was used to determine differentially expressed genes between the patient with neurotoxicity and all other patients. Differential expression was determined with a two-sided Mann–Whitney *U*-test, and *P* values were corrected using the Benjamini–Hochberg method.

Immunohistochemistry. Slides with 5-µm sections from paraffin-embedded tissues from autopsies were stained with CD3 (LN10) and GFAP (GA5) pre-diluted BOND reagents from Leica Biosystems, heat-induced epitope retrieval for 20 min with ER2 (Bond Epitope Retrieval Solution 2), MSMC DAB detection and counterstained per established staining protocol on the automated Leica Biosystems BOND-III platform. Immunohistochemistry for BCMA was performed using Ventana DISCOVERY ULTRA from Roche. This system allows for automated baking, de-paraffinization and cell conditioning. Semi-automatic staining was performed using BCMA antibody (cat. no. B0807 from USBiological) at 1:10 dilution during 60 min. As secondary antibody, Discovery OmniMap anti-rabbit-HRP from Roche (760-4310) was used, and the signal was obtained using DISCOVERY ChromoMap DAB RUO from Roche (760-2513) (brown signal). Tissues were counterstained with hematoxylin (in blue).

Analysis of public datasets. The mRNA expression data from the Allen Brain Atlas were last accessed on 25 April 2021. The heat map can be found at http://human.brain-map.org/ (human brain data) when doing a Gene Search for *TNFRSF17* and *DRD1* and selecting 'View Selection Thumbnails'. Raw expression data of the heat map used as part of the figures were downloaded by the authors from the Allen Brain Atlas data portal and are included as Source Data of Extended Data Fig. 8.

Reporting Summary. Further information on research design is available in the Nature Research Reporting Summary linked to this article.

Data availability

All requests for raw and analyzed data and materials will be promptly reviewed by the Icahn School of Medicine at Mount Sinai and Mount Sinai Hospital to determine if the request is subject to any confidentiality and data protection obligations. Requests for data should be addressed to the corresponding author via e-mail, and a reply will be sent within ten business days. Any data and materials that can be shared will be released via a material transfer agreement. Raw and analyzed CITE-seq data are available through the National Center for Biotechnology Information's Gene Expression Omnibus (accession no. GSE182527). Mass cytometry and intracellular cytokine data are available through the FlowRepository website (ID FR-FCM-Z4KB). The images derived from the Allen Human Brain Atlas can be accessed at https://human.brain-map.org/. Specific URLs to recreate the following figures are provided: Fig. 2b (https://human.brain-map.org/static/brainexplorer), Extended Data Fig. 8a (https://human.brain-map.org/microarray/search/show?search_type=user_selections&user_selection_mode=1) and Extended Data Fig. 8b (https://human.brain-map.org/microarray/gene/show/605), and source data are available. For all clinical measurements and cytokine levels (Extended Data Figs. 1, 2, 6 and 9d–f), source data are available. Source data are provided with this paper. Q10

References

21. Kotecha, N., Krutzik, P. O. & Irish, J. M. Web-based analysis and publication of flow cytometry experiments. *Curr. Protoc. Cytom.* **Chapter 10**, Unit10.17 (2010).
22. Kolde, R. pheatmap: Pretty Heatmaps. Version 1.0.12. https://rdrr.io/cran/pheatmap/ (2019).
23. Wickham, H. *ggplot2: Elegant Graphics for Data Analysis*, (Springer-Verlag, 2016).
24. Zunder, E. R. et al. Palladium-based mass tag cell barcoding with a doublet-filtering scheme and single-cell deconvolution algorithm. *Nat. Protoc.* **10**, 316–333 (2015).
25. Nowicka, M. et al. CyTOF workflow: differential discovery in high-throughput high-dimensional cytometry datasets. *F1000Res* **6**, 748 (2017).
26. Weber, L. M. diffcyt: Differential discovery in high-dimensional cytometry via high-resolution clustering. *Commun. Biol.* **2**, 183 (2019).
27. Crowell, H. L., Zanotelli, V. R. T., Chevrier, S. & Robinson, M. D. CATALYST: Cytometry dATa anALYSis Tools. https://github.com/HelenaLC/CATALYST (2020). Q12
28. Ellis, B. et al. flowCore: basic structures for flow cytometry data. https://www.bioconductor.org/packages/devel/bioc/manuals/flowCore/man/flowCore.pdf (2019).
29. Van Gassen, S. et al. FlowSOM: using self-organizing maps for visualization and interpretation of cytometry data. *Cytometry A* **87**, 636–645 (2015).
30. Kim, H. J., Lin, Y., Geddes, T. A., Yang, J. Y. H. & Yang, P. CiteFuse enables multi-modal analysis of CITE-seq data. *Bioinformatics* **36**, 4137–4143 (2020).
31. Amezquita, R. A. et al. Orchestrating single-cell analysis with Bioconductor. *Nat. Methods* **17**, 137–145 (2019).

Acknowledgements

The authors would like to thank T. Dawson, H. Xie, M. Patel and the rest of the staff members at the Human Immune Monitoring Center at the Icahn School of Medicine for sample management and their help conducting omics assays. Furthermore, we would like to thank M. Garcia-Barros and R. Brody from the Biorepository and Pathology Core at the Icahn School of Medicine for immunohistochemistry staining. S.P. acknowledges support by the National Cancer Institute (NCI) (R01 CA244899 and R01 CA252222) and receives research funding from Amgen, Celgene/Bristol Myers Squibb and Karyopharm. M.M. acknowledges support from the National Institute of Allergy and Infectious Diseases (U24 AI118644-05S1, U19 AI128949 and U19 AI118610), from the NCI (R01 CA254104, R01 CA257195 and P30 CA196521-05S2), from a Fast Grant (George Mason University), from the Gates Foundation and from the Samuel Waxman Cancer Research Foundation. J.B. acknowledges support from the NCI (R01 CA246239-01). Q9

Author contributions

S.P. provided investigation, conceptualization, methodology, analysis, resources and supervision review as well as edits of the manuscript. D.M., S.G., C.B.S., S.J. and S.P. were involved in different aspects of clinical care for the patient, including interpretation of imaging. O.V.O., A.A., B.U., S.K.S., A.R., J.D.B., M.M. and S.P. were involved in design, execution, interpretation and analysis of immunological and genomics assays. S.S., J.F.C., J.T.F. and M.F. were involved in design, execution, interpretation and analysis of (neuro)pathological studies. O.V.O., A.A., A.L. and S.P. conducted data analysis, including creation of figures. O.V.O., A.A., J.D.B., M.M., S.J. and S.P. contributed to the writing of the first manuscript draft, which was approved and edited by all co-authors.

Competing interests

O.V.O. has no relevant conflicts to disclose. A.A. has no relevant conflicts to disclose. B.U. has no relevant conflicts to disclose. S.S. has no relevant conflicts to disclose. S.S. is currently employed by Sema4 but was not working for the company at the time of preparation of the manuscript. D.M. has worked as a consultant for Bristol Myers Squibb, Celgene, Foundation Medicine, GSK, Janssen, Kinevant and Sanofi and has received grant and research support from Allogene, Amgen, Bristol Myers Squibb, Celgene, Janssen and Regeneron. D.M. is currently employed by Johnson & Johnson but was not working for the company at the time of preparation of the manuscript. S.G. has no relevant conflicts to disclose. J.T.F. has no relevant conflicts to disclose. J.F.C. has no relevant conflicts to disclose. C.B.S. is a member of the ciltacabtagene autoleucel Risk Evaluation and Mitigation Strategy advisory board. S.K.S. has no relevant conflicts to disclose. A.R. is currently employed by Immunai but was not working for the company at the time of preparation of the manuscript. A.L. has no relevant conflicts to disclose. J.D.B. has received consulting fees from Celldex, Genentech, Gilead, Janssen, Kite and Merck and has received research funding or reagents provided by Celldex, Genentech, Janssen, Kite and Merck. M.M. has no relevant conflicts to disclose. S.J. is a consultant for Bristol Myers Squibb, Janssen, Karyopharm, Merck, Sanofi and Takeda. S.P. receives research funding from Amgen, Celgene/Bristol Myers Squibb and Karyopharm and consulting fees from Foundation Medicine. All other authors declare no competing interests. Q11

Additional information

Extended data is available for this paper at https://doi.org/10.1038/s41591-021-01564-7.

Supplementary information The online version contains supplementary material available at https://doi.org/10.1038/s41591-021-01564-7.

Correspondence and requests for materials should be addressed to Samir Parekh.

Peer review information *Nature Medicine* thanks Leo Rasche, Eric Smith, Daniel Rubin and the other, anonymous, reviewer(s) for their contribution to the peer review of this work. Saheli Sadanand was the primary editor on this article and managed its editorial process and peer review in collaboration with the rest of the editorial team.

Reprints and permissions information is available at www.nature.com/reprints.

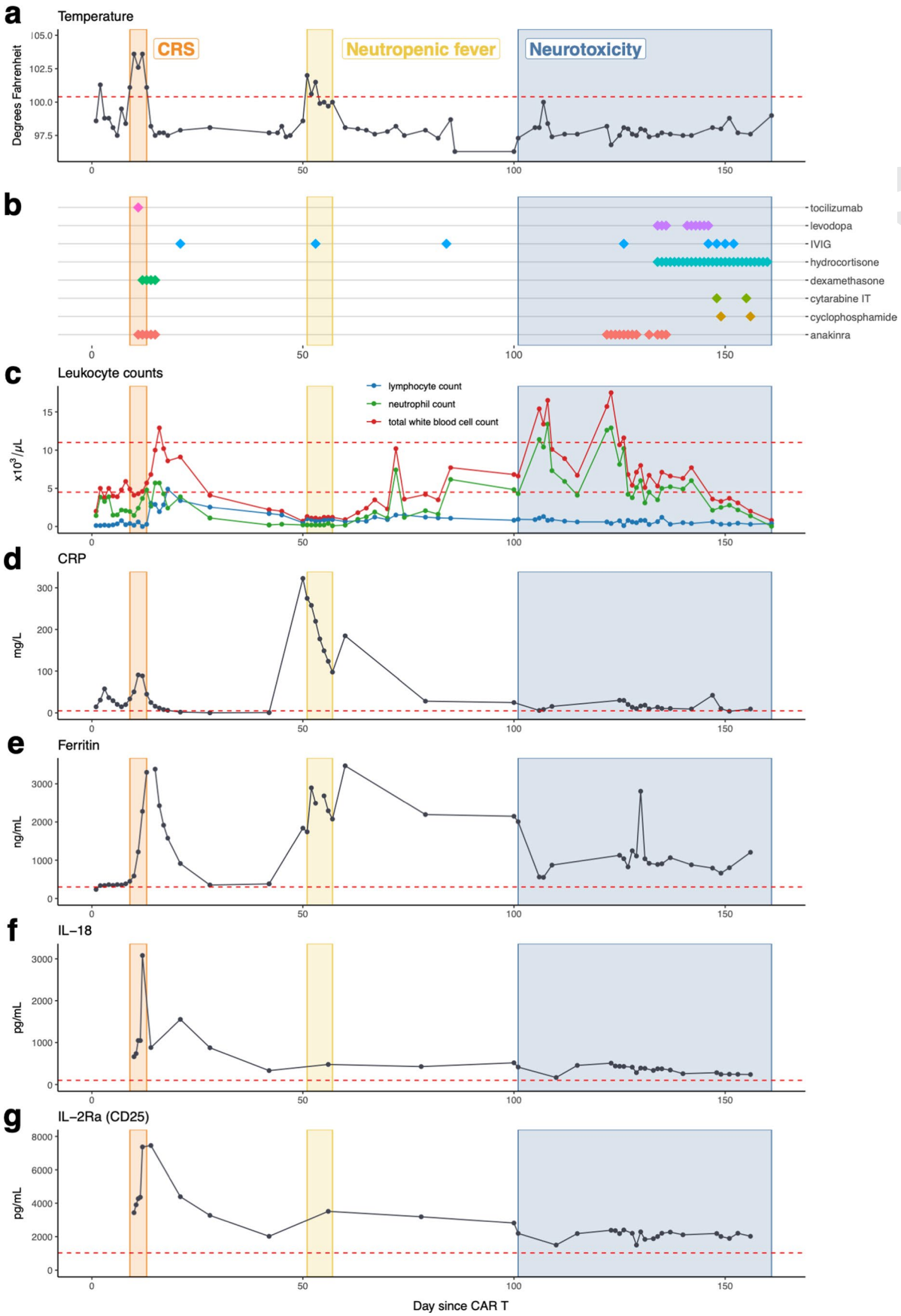

Extended Data Fig. 1 | See next page for caption.

Extended Data Fig. 1 | Clinical course and biochemical parameters after CAR-T cell treatment. The time periods associated with cytokine release syndrome (CRS), neutropenic fever and neurotoxicity are annotated in the individual subplots. All cytokine levels were determined in the peripheral blood. **(a)** Temperature curve. **(b)** Administration of relevant pharmacologic treatments during the period after CAR-T treatment. **(c)** Total leukocyte, lymphocyte, and neutrophil counts. **(d)** Time course of CRP level (mg/L). **(e)** Time course of ferritin level (ng/mL). **(f)** Time course of IL-18 level (pg/mL). **(g)** Time course of IL-2Ra (CD25) level (pg/mL).

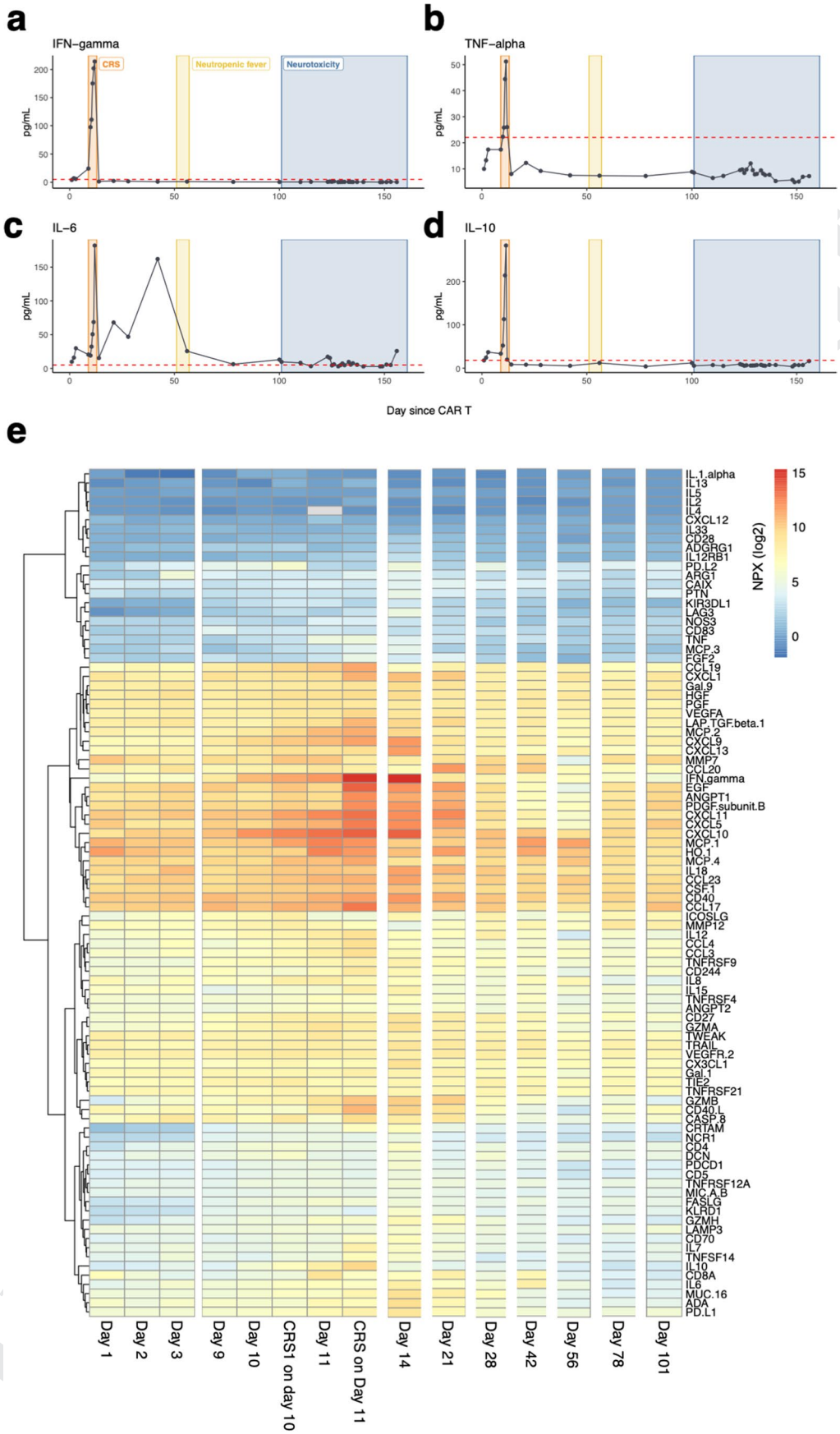

Extended Data Fig. 2 | See next page for caption.

Extended Data Fig. 2 | Cytokine levels and time course after CAR-T cell treatment. The time periods associated with cytokine release syndrome (CRS), neutropenic fever and neurotoxicity are annotated in the individual subplots. **(a)** Time course of IFN-gamma level (pg/mL). **(b)** Time course of TNF-alpha level (pg/mL). **(c)** Time course of IL-6 level (pg/mL). **(d)** Time course of IL-10 level (pg/mL). All measurements are from peripheral blood plasma. **(e)** Olink cytokine profiling of peripheral blood plasma at different time points after chimeric antigen receptor (CAR) T cell therapy. Values shown are normalized protein expression (NPX) values according the Olink protocol in log2 scale (high protein levels in red, low protein levels in blue).

a

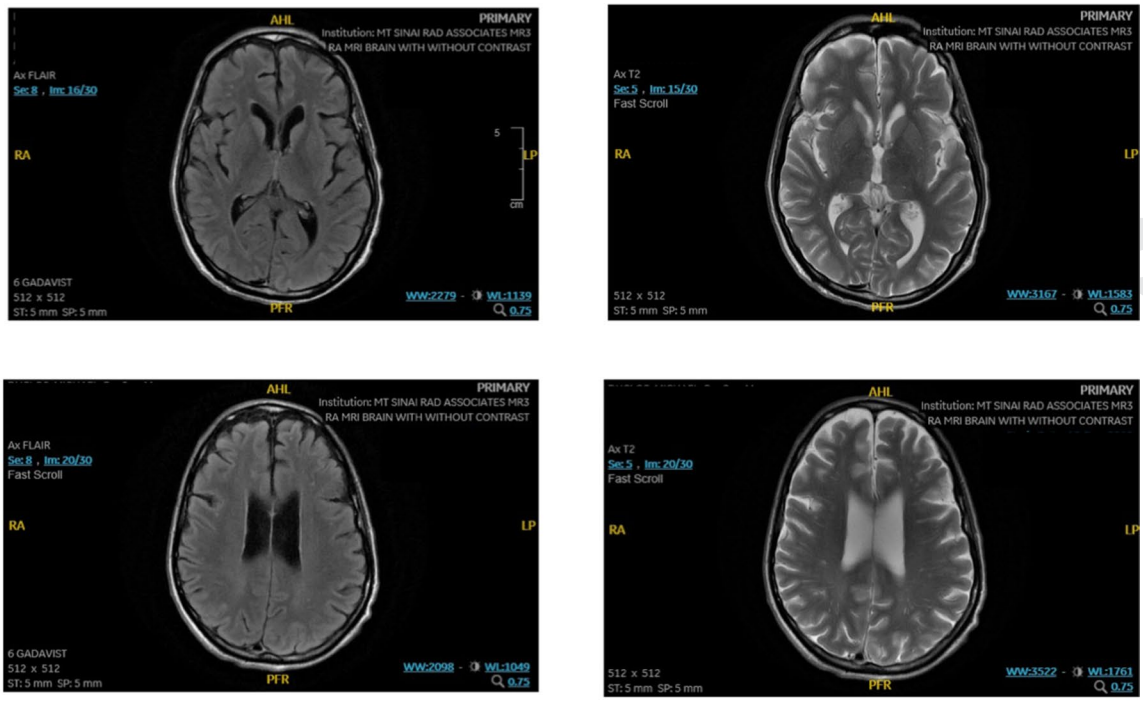

b

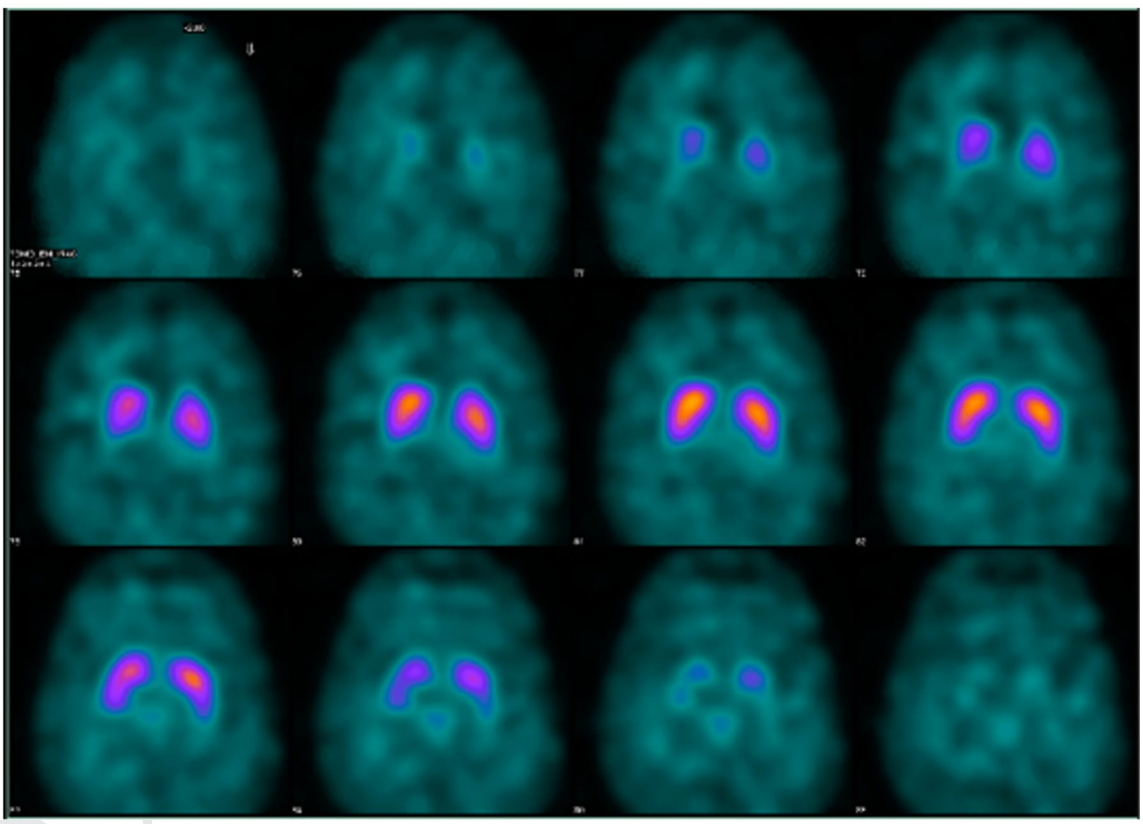

Extended Data Fig. 3 | MRI and Ioflupane single photon emission computed tomography imaging after the onset of neurotoxicity. (a) MRI axial FLAIR (left) and T2 (right) images at the level of the deep brain nuclei (top) and the cerebral cortex (top), conducted at day 101 after CAR-T infusion. Images demonstrate small punctuate hyperintensities present on imaging prior to CAR-T therapy and putatively due to pre-existing microvascular damage. **(b)** Ioflupane (123-I) scan images, conducted at day 155 after CAR-T infusion, show normal uptake at the level of the basal ganglia.

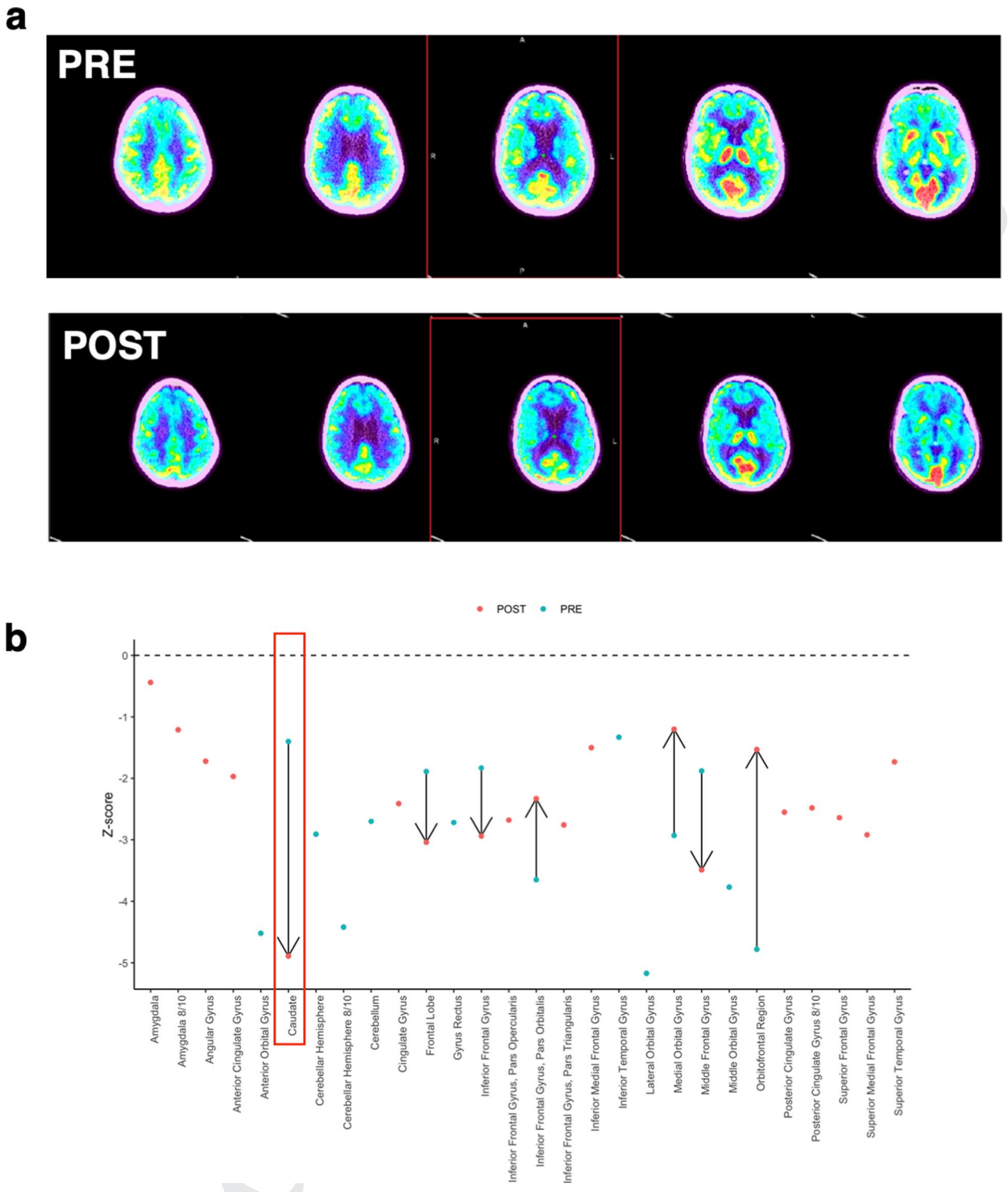

Extended Data Fig. 4 | Quantitative analysis of FDG-PET/CT images confirms decreased metabolism in caudate nucleus after CAR-T cell therapy. **(a)** FDG-PET axial splash images pre (top) and post (bottom) CAR-T infusion. Shown is a spectral scale with high metabolism/perfusion in red, to low metabolism/perfusion in dark blue. **(b)** Quantitative analysis showing normalized Z-score for all available regions of the brain before (blue) and after (red) CAR-T infusion. The caudate is highlighted. The normalized score was calculated using MIMneuro, comparing the image with a library of 43 FDG neurologic controls (41-80 years old).

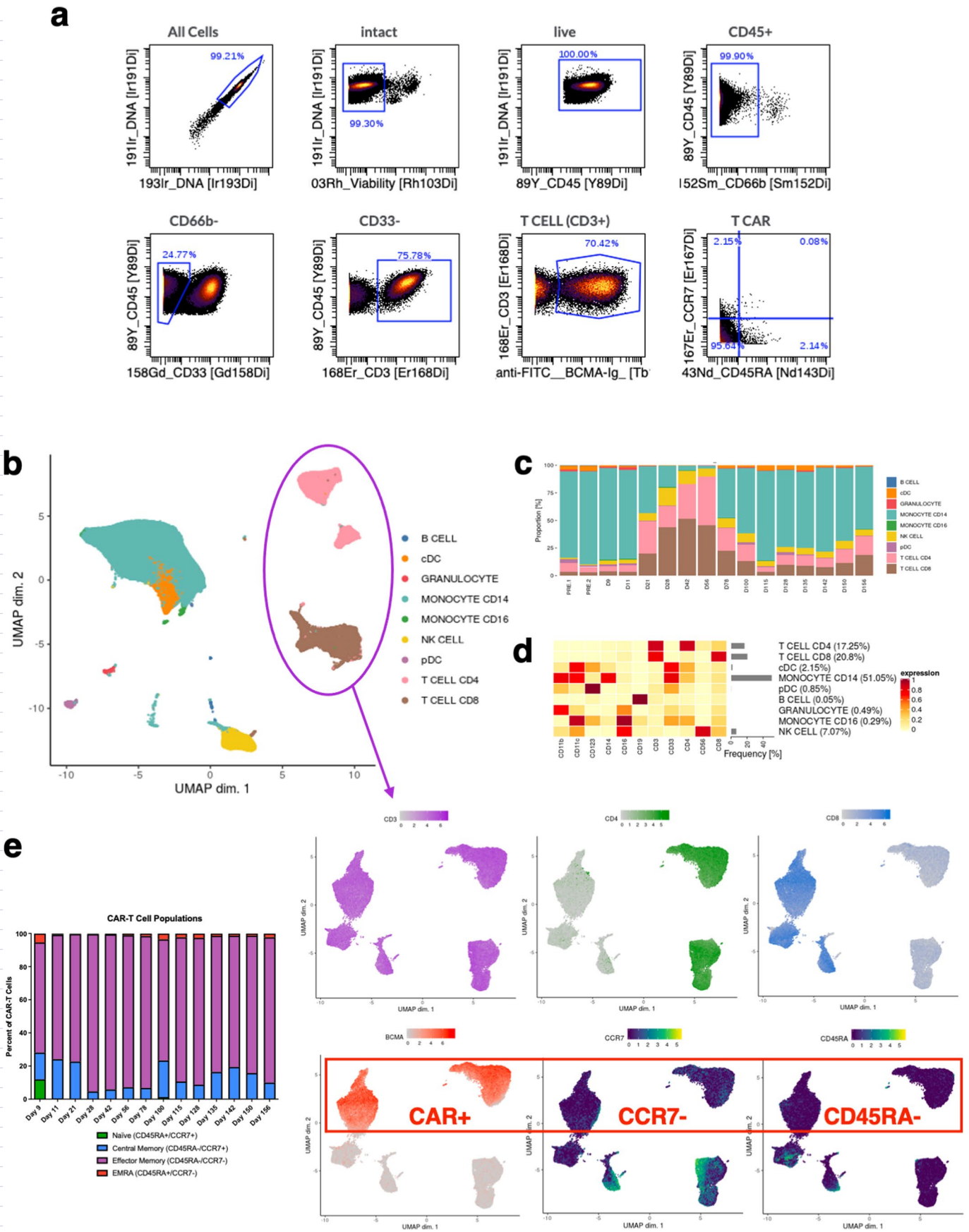

Extended Data Fig. 5 | See next page for caption.

Extended Data Fig. 5 | Mass cytometry characterizes the effector-memory phenotype of CAR-T cells over time. (a) Representative mass cytometry (CyTOF) plots illustrating the gating strategy for identifying CAR-T cells and T cell subsets as shown in Figs. 1a, 1d and Extended Data Figure 5e. **(b)** UMAP representation of peripheral blood mononuclear cells (PBMC) collected at time points shown in **(a)** shows the clustering of major immune cell types. **(c)** Relative contribution of major immune cell types in samples at different time points. **(d)** Expression of canonical markers, showing accurate classification of major immune cell types. **(e)** CAR-T cell phenotype, as determined by expression of CCR7 and CD45RA, illustrating a high fraction of effector-memory T cells at all time points. Each bar corresponds to N = 1 sample collected from the patient. The UMAP plots visually illustrate the clustering of T cells and confirm low CCR7 and CD45RA expression on CAR-T cells.

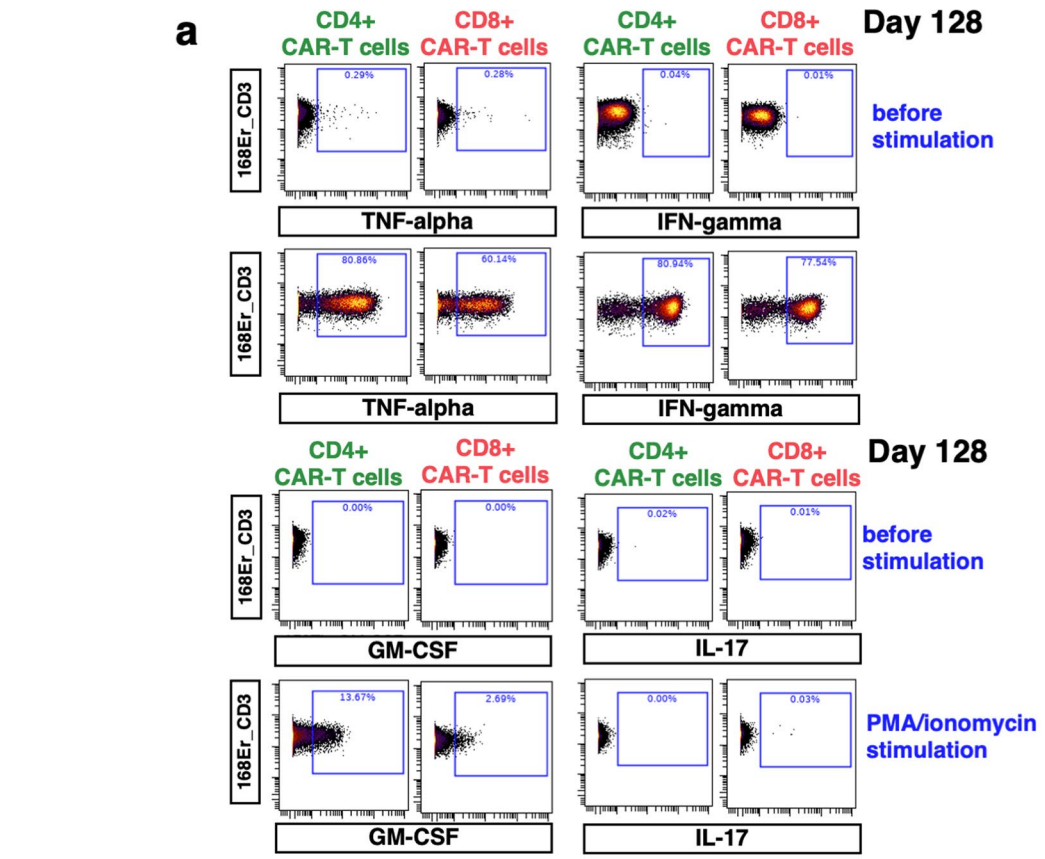

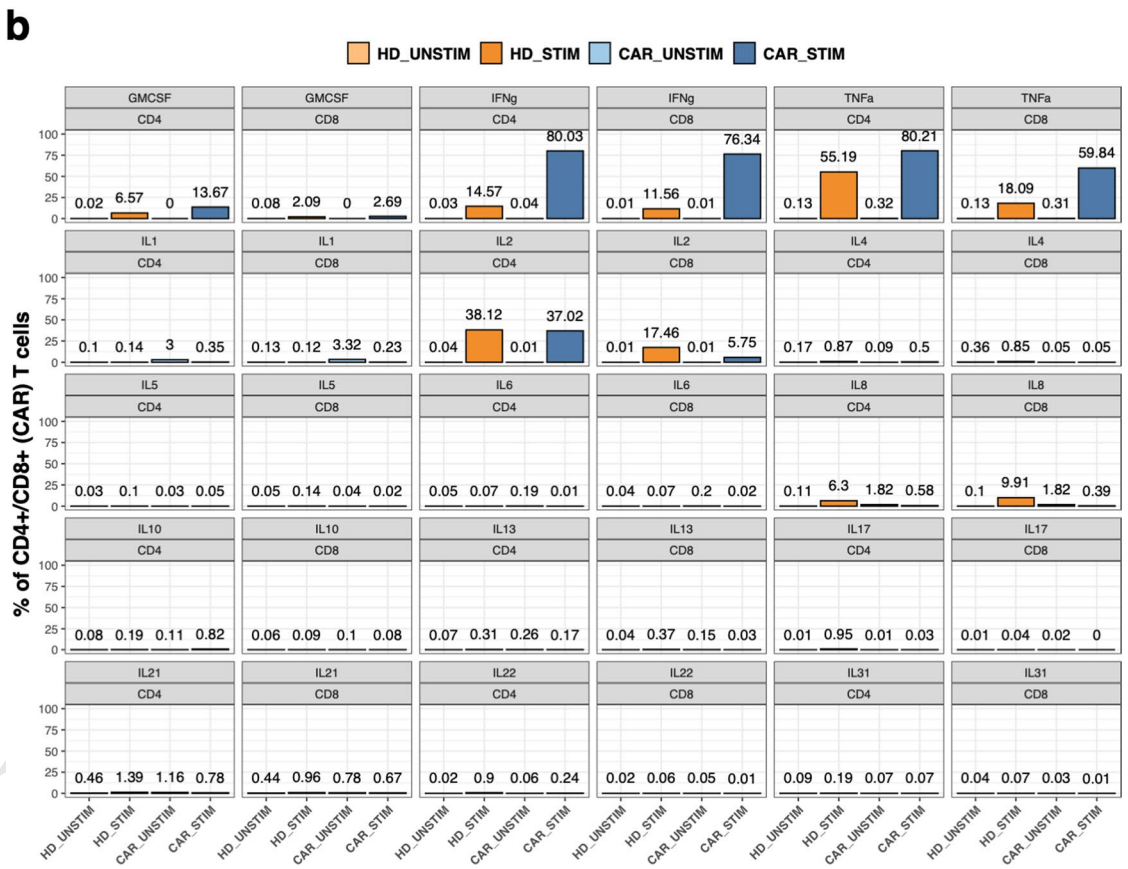

Extended Data Fig. 6 | See next page for caption.

Extended Data Fig. 6 | Cytokine expression of peripheral blood CAR-T cells isolated at day 128 after treatment vs. healthy donor T cells. (a) CAR-T cells isolated at day 128 after CAR-T infusion were stimulated with PMA/ionomycin and cytokine production was assessed with mass cytometry. Shown here is high expression of TNF-alpha, interferon-gamma and GM-CSF and lack of expression of IL-17 in CD4 + (left) and CD8 + (right) CAR-T cells. **(b)** Percentage of CAR-T cells (orange) and healthy donor (HD) T cells (blue) expressing the full set of cytokines tested before (UNSTIM) or after (STIM) stimulation with PMA/ionomycin. Each bar represents N = 1 sample analyzed from the patient or healthy donor.

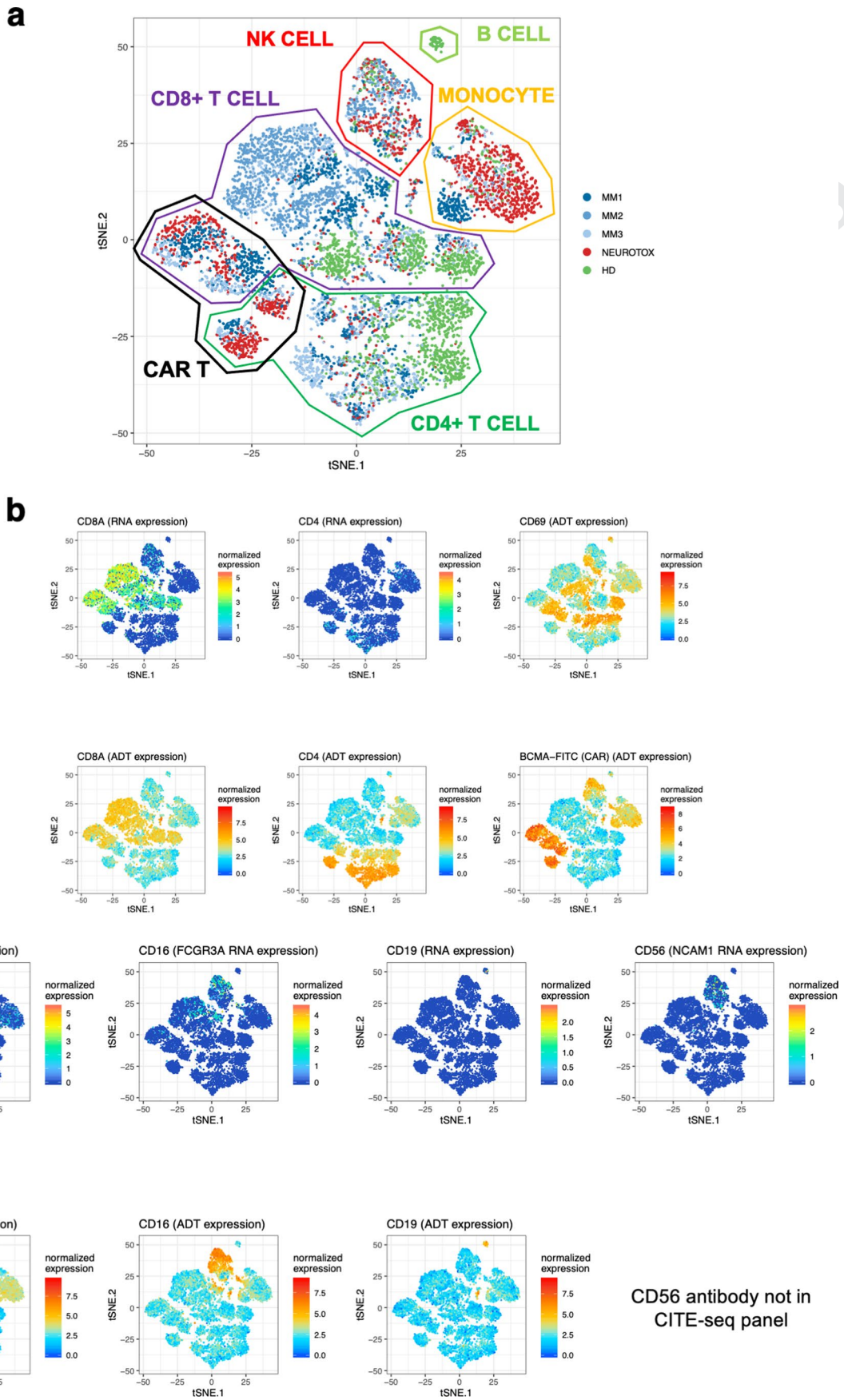

Extended Data Fig. 7 | See next page for caption.

Extended Data Fig. 7 | Expression of canonical markers on CITE-seq data identifies and clusters major immune cell types. (a) t-SNE plot representation of CITE-seq analysis of peripheral blood mononuclear cells before and after PMA/ionomycin stimulation. Clustering was determined by similarity network fusion (SNF) and Louvain clustering algorithm. Individual cells are colored by subject (healthy donor (HD), neurotoxicity patient (NEUROTOX) and 3 other patients on the same clinical trial without neurotoxicity (MM1, MM2, MM3). Highlighted are the major immune cell types (B cells, NK cells, CD8 + T cells, CD4 + T cells, CAR-T cells and monocytes). There is a small cluster of events that corresponds to multiplets or debris (centrally, not highlighted). **(b)** Expression level of canonical genes: *CD8A*, *CD4*, *CD14*, *FCGR3A* (CD16), *CD19* and *NCAM1* (CD56). In each case showing both mRNA (top) and ADT (antibody-derived tag, representation of protein level) (high = red, low = blue). Expression levels are normalized as described in the Methods.

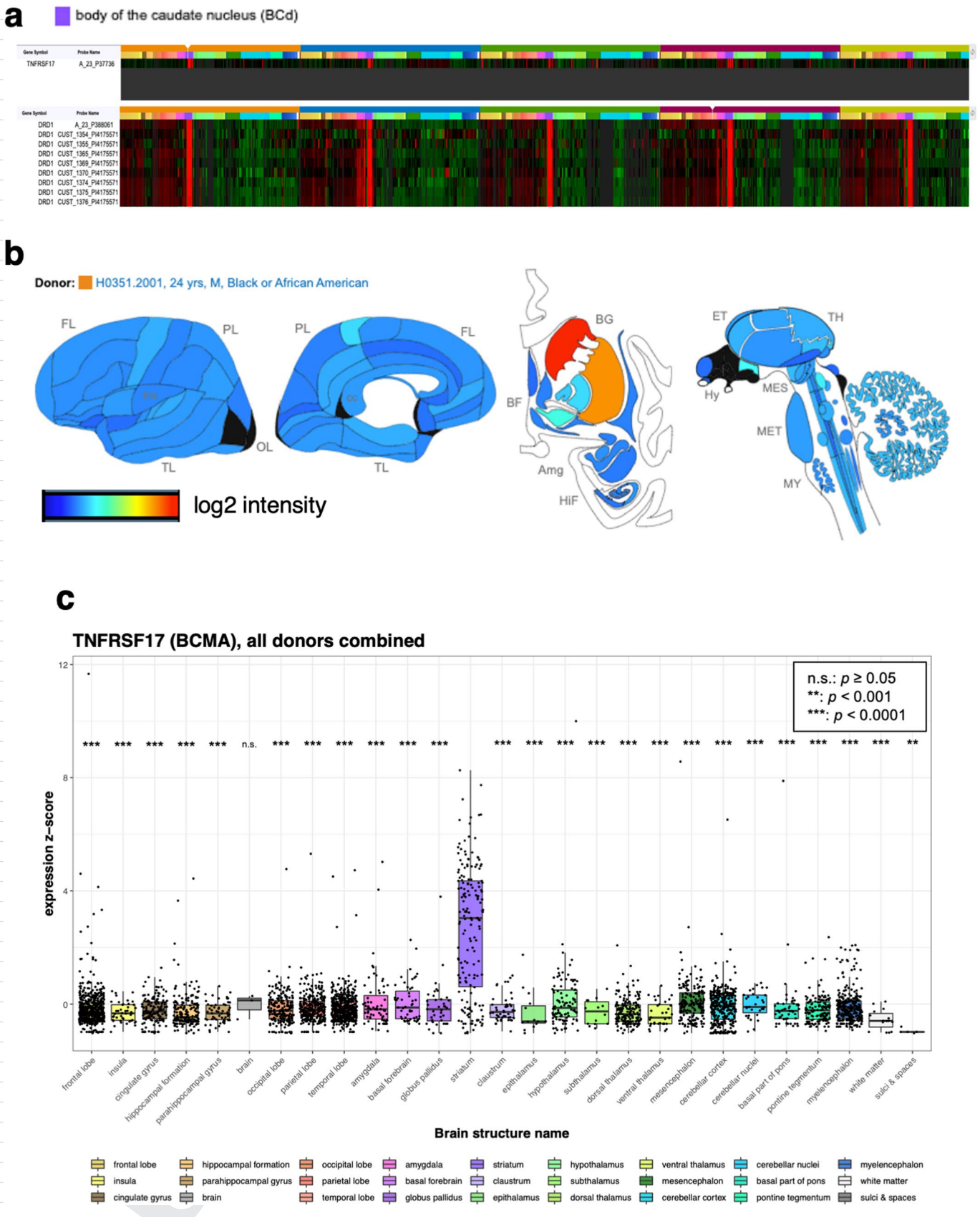

Extended Data Fig. 8 | See next page for caption.

Extended Data Fig. 8 | Expression of BCMA in healthy donors of the Allen Brain Atlas and presence of CAR-T cells in CSF of patient. (a) Microarray data on top illustrates the expression of *TNFRSF17* (BCMA) in the caudate nucleus of 5 healthy brain donors. The bottom shows that regions of *TNFRSF17* (BCMA) expression coincides with *DRD1* (dopamine receptor D1) expression, a protein know to be highly specific for the caudate nucleus. Image credit: Allen Institute: © 2010 Allen Institute for Brain Science. Allen Human Brain Atlas; available from: human.brain-map.org. **(b)** Schematic representation showing the log2 intensity of *TNFRSF17* (BCMA) RNA expression in a single patient from the Allen Brain Atlas. Image credit: Allen Institute: © 2010 Allen Institute for Brain Science. Allen Human Brain Atlas; available from: human.brain-map.org. **(c)** Quantitative representation of the Allen Brain Atlas data with boxplots (median, Q1 and Q3 quartiles, whiskers up to 1.5 x IQR) showing normalized expression (z-score) across all six donors for different brain structures (N = 6, total of 3,702 probes across 27 brain regions). The *p*-values shown correspond to a two-sided Mann-Whitney *U* test of striatum versus any other region (**: $p < 0.001$, ***: $p < 0.0001$, n.s.: $p \geq 0.05$).

A B

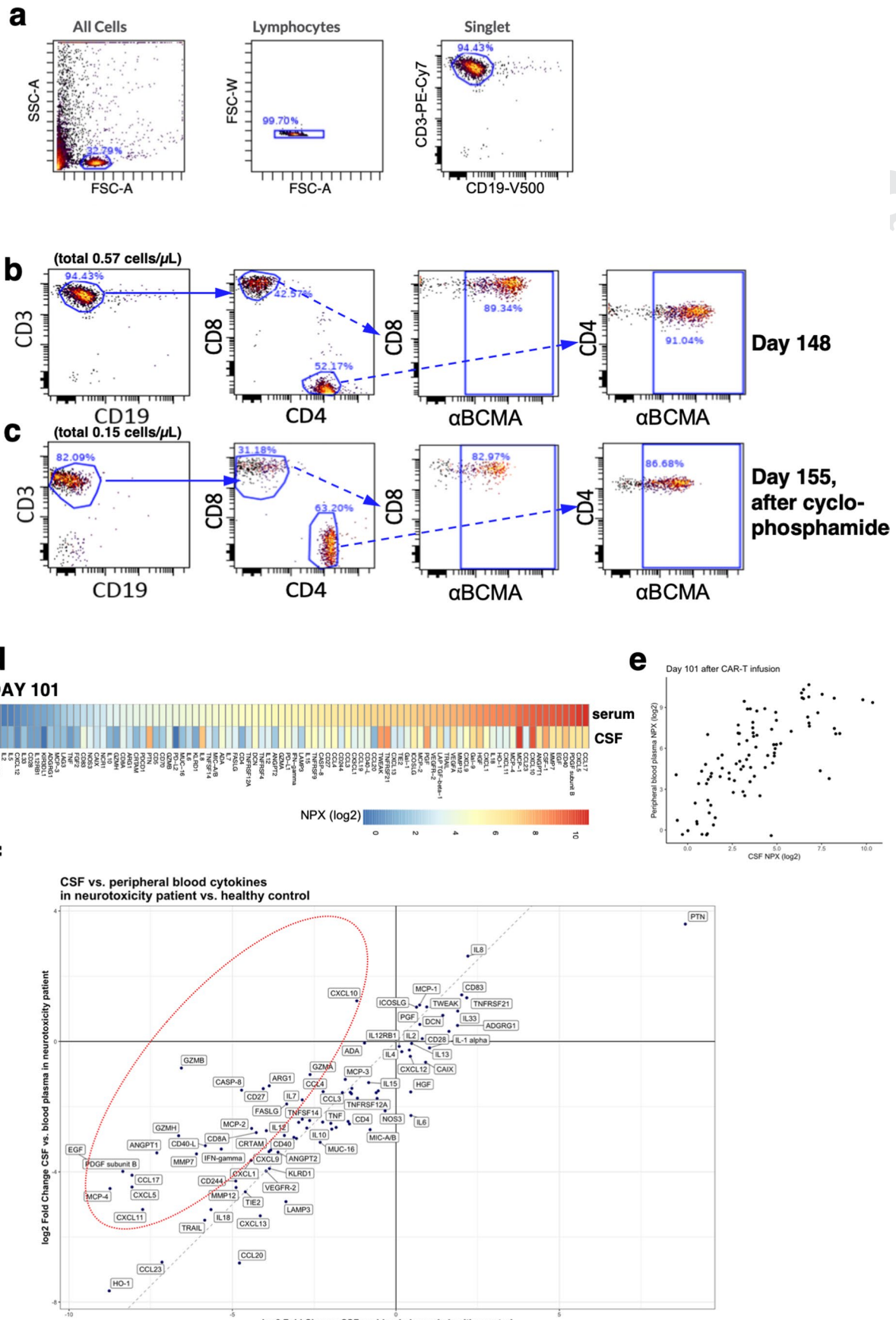

Extended Data Fig. 9 | See next page for caption.

Extended Data Fig. 9 | Presence and persistence of CAR-T cells in CSF of patient and cytokine profiling in peripheral blood plasma versus CSF after development of neurotoxicity. (a) Representative plots showing the gating strategy on CSF to get to the T cell gate. **(b)** Flow cytometric data of cerebrospinal fluid from day 148 after CAR-T cell infusion, showing presence of CD4 + and CD8 + CAR-T cells. **(c)** Flow cytometric data of cerebrospinal fluid from day 155 after CAR-T cell infusion (that is after administration of intravenous cyclophosphamide and intrathecal cytarabine), showing persistent presence of CD4 + and CD8 + CAR-T cells. **(d)** Normalized protein expression (NPX) log2 values of all cytokines in the Olink Immuno-Oncology panel, in serum (top) and CSF (bottom) (high protein levels in red, low protein levels in blue). **(e)** Scatter plot showing overall correlation of cytokine levels in plasma versus CSF (Pearson correlation coefficient $r = 0.70$, two-sided $p < 0.001$). **(f)** The log2 fold change (FC) of CSF versus blood plasma in a healthy control (along *x*-axis) and the patient who developed neurotoxicity (along *y*-axis). Highlighted are a selection of cytokines that are overrepresented in the patient's CSF compared to the healthy control data. Among the cytokines that are overrepresented, we note a set of cytokines suggesting T cell activation (for example GZMB, GZMA, IFN-γ, CD40L, CD8A, CD27, FASLG), cytokines that are induced by IFN-γ (for example CXCL5, CXCL10, CXCL11) and that are known to act as chemo-attractants for T cells (among other immune cell types), and cytokines that point to possible involvement of cells in the blood-brain barrier (BBB) (for example PDGFb, EGF and ANGPT1).

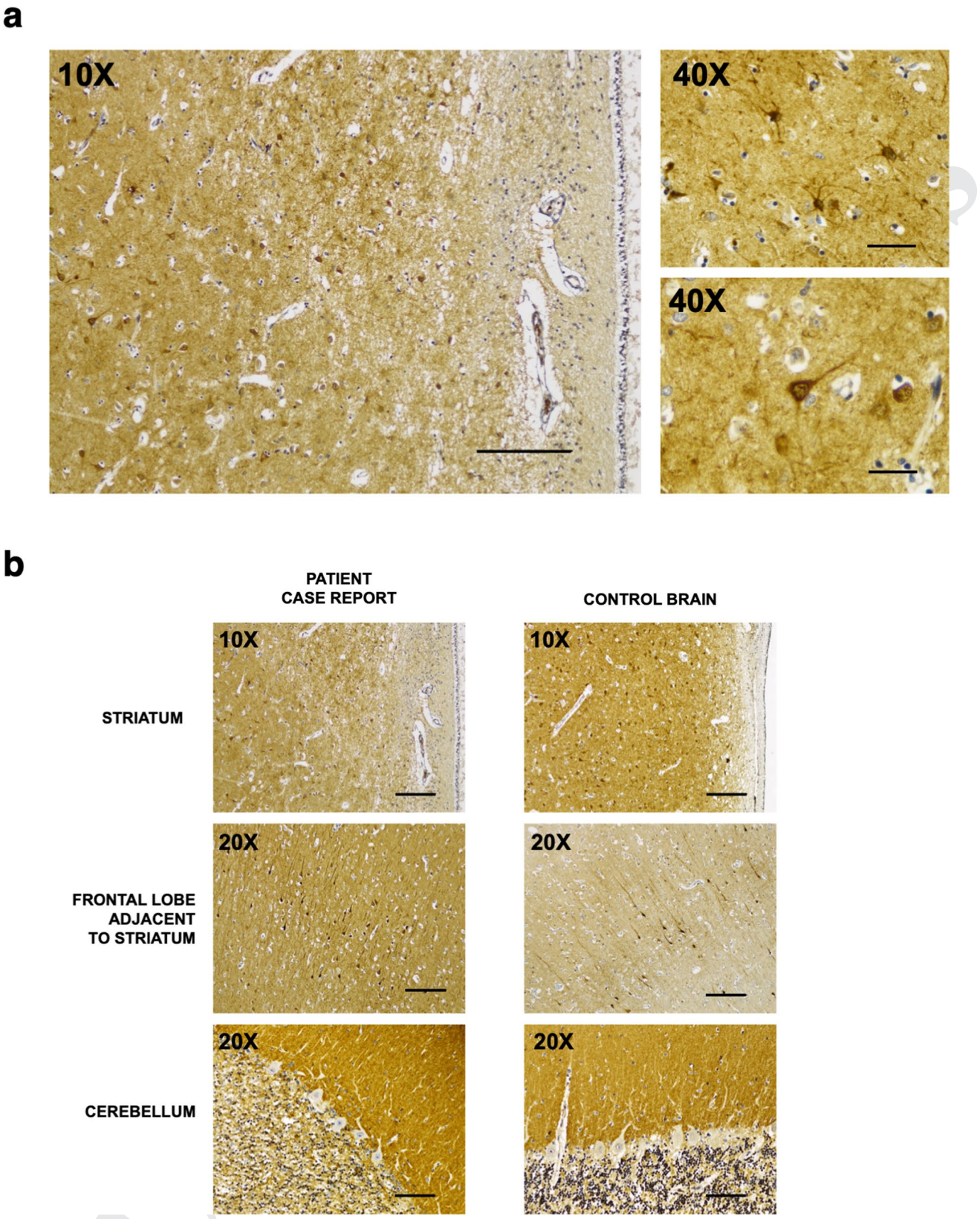

Extended Data Fig. 10 | See next page for caption.

Extended Data Fig. 10 | Immunohistochemistry showing BCMA protein expression in brain tissue of the patient and in a control brain. (a) BCMA immunohistochemistry of the caudate nucleus subependymal region (10x magnification, left, scale bar 200 μm). Inset (40x magnification, right, scale bar 50 μm) shows high magnification image of astrocytes (top) and a neuron (bottom) that stained positive for BCMA, whereas surrounding cells were negative. Images shown are representative slides from the caudate nucleus from the patient described in this case report (N = 1). For each region stained, at least 3 slides were available. **(b)** BCMA immunohistochemistry of selected brain regions as annotated in the patient of interest (left) versus a control brain (right) from a subject who died due to non-neurologic illness (10x magnification (top), scale bar 200 μm and 20x magnification (middle, bottom), scale bar 100 μm). Images shown are representative slides from the patient described in this case report (N = 1), as well as a single control brain (N = 1). For each region stained, at least 3 slides were available. The experiment was repeated in a second control brain with similar results.

QUERY FORM

Nature Medicine	
Manuscript ID	**[Art. Id: 1564]**
Author	**Oliver Van Oekelen**

AUTHOR:

The following queries have arisen during the editing of your manuscript. Please answer by making the requisite corrections directly in the e.proofing tool rather than marking them up on the PDF. This will ensure that your corrections are incorporated accurately and that your paper is published as quickly as possible.

Query No.	*Nature of Query*
Q1:	Please note that affiliations have been re-numbered for sequential order.
Q2:	Please check your article carefully, coordinate with any co-authors and enter all final edits clearly in the eproof, remembering to save frequently. Once corrections are submitted, we cannot routinely make further changes to the article.
Q3:	Note that the eproof should be amended in only one browser window at any one time; otherwise changes will be overwritten.
Q4:	Author surnames have been highlighted. Please check these carefully and adjust if the first name or surname is marked up incorrectly. Note that changes here will affect indexing of your article in public repositories such as PubMed. Also, carefully check the spelling and numbering of all author names and affiliations, and the corresponding email address(es).
Q5:	You cannot alter accepted Supplementary Information files except for critical changes to scientific content. If you do resupply any files, please also provide a brief (but complete) list of changes. If these are not considered scientific changes, any altered Supplementary files will not be used, only the originally accepted version will be published.
Q6:	If applicable, please ensure that any accession codes and datasets whose DOIs or other identifiers are mentioned in the paper are scheduled for public release as soon as possible, we recommend within a few days of submitting your proof, and update the database record with publication details from this article once available.
Q7:	Your paper has been copy edited. Please review every sentence to ensure that it conveys your intended meaning; if changes are required, please provide further clarification rather than reverting to the original text. Please note that formatting (including hyphenation, Latin words, and any reference citations that might be mistaken for exponents) has been made consistent with our house style.
Q8:	Please ensure that genes are correctly distinguished from gene products: for genes, official gene symbols (e.g., NCBI Gene) for the relevant species should be used and italicized; gene products such as proteins and noncoding RNAs should not be italicized. Please check the figures, too.
Q9:	Please check that all funders have been appropriately acknowledged and that all grant numbers are correct.
Q10:	If applicable, please ensure accession codes are scheduled for release on or before this article's scheduled publication date and update the database record with publication details from this article once available.

QUERY FORM

Nature Medicine	
Manuscript ID	**[Art. Id: 1564]**
Author	**Oliver Van Oekelen**

AUTHOR:

The following queries have arisen during the editing of your manuscript. Please answer by making the requisite corrections directly in the e.proofing tool rather than marking them up on the PDF. This will ensure that your corrections are incorporated accurately and that your paper is published as quickly as possible.

Query No.	*Nature of Query*
Q11:	Please check that the Competing Interests declaration is correct as stated. If you declare competing interests, please check the full text of the declaration for accuracy and completeness.
Q12:	Please confirm the correct URL for Ref. 27

nature research

Corresponding author(s): Samir Parekh

Last updated by author(s): Sep 22, 2021

Reporting Summary

Nature Research wishes to improve the reproducibility of the work that we publish. This form provides structure for consistency and transparency in reporting. For further information on Nature Research policies, see our Editorial Policies and the Editorial Policy Checklist.

Statistics

For all statistical analyses, confirm that the following items are present in the figure legend, table legend, main text, or Methods section.

n/a	Confirmed
☐	☒ The exact sample size (*n*) for each experimental group/condition, given as a discrete number and unit of measurement
☐	☒ A statement on whether measurements were taken from distinct samples or whether the same sample was measured repeatedly
☐	☒ The statistical test(s) used AND whether they are one- or two-sided *Only common tests should be described solely by name; describe more complex techniques in the Methods section.*
☒	☐ A description of all covariates tested
☐	☒ A description of any assumptions or corrections, such as tests of normality and adjustment for multiple comparisons
☐	☒ A full description of the statistical parameters including central tendency (e.g. means) or other basic estimates (e.g. regression coefficient) AND variation (e.g. standard deviation) or associated estimates of uncertainty (e.g. confidence intervals)
☐	☒ For null hypothesis testing, the test statistic (e.g. *F*, *t*, *r*) with confidence intervals, effect sizes, degrees of freedom and *P* value noted *Give P values as exact values whenever suitable.*
☒	☐ For Bayesian analysis, information on the choice of priors and Markov chain Monte Carlo settings
☒	☐ For hierarchical and complex designs, identification of the appropriate level for tests and full reporting of outcomes
☐	☒ Estimates of effect sizes (e.g. Cohen's *d*, Pearson's *r*), indicating how they were calculated

Our web collection on statistics for biologists contains articles on many of the points above.

Software and code

Policy information about availability of computer code

Data collection	Next generation sequencing was collected by Illumina Nextseq (CITE-seq data). Mass cytometry (CyTOF) data was collected on the Fluidigm CyTOF2 system. Flow cytometry data was acquired on the BD FACS LSR Fortessa flow cytometry system (BD Biosciences).
Data analysis	Following software and packages were used (with respective version where applicable): Mass cytometry data analysis: Cytobank, R (3.6.1), CATALYST (1.14.0), flowCore (2.2.0), diffcyt (1.10.0) Flow Cytometry data analysis: Cytobank CITE-seq analysis: Cellranger (3.0.1), R (3.6.1), Citefuse (1.2.0)

For manuscripts utilizing custom algorithms or software that are central to the research but not yet described in published literature, software must be made available to editors and reviewers. We strongly encourage code deposition in a community repository (e.g. GitHub). See the Nature Research guidelines for submitting code & software for further information.

Data

Policy information about availability of data

All manuscripts must include a data availability statement. This statement should provide the following information, where applicable:

- Accession codes, unique identifiers, or web links for publicly available datasets
- A list of figures that have associated raw data
- A description of any restrictions on data availability

All requests for raw and analyzed data and materials will be promptly reviewed by the Icahn School of Medicine at Mount Sinai and the Mount Sinai Hospital to verify if the request is subject to any confidentiality and data protection obligations. Requests for data should be addressed to the corresponding author via e-mail and will receive a reply within 10 business days. Any data and materials that can be shared will be released via a material transfer agreement. Raw and analyzed CITE-seq data are available through the National Center for Biotechnology Information (NCBI) Gene Expression Omnibus (GEO) (accession no. GSE182527). Mass

cytometry and intracellular cytokine data are available through the FlowRepository website (ID FR-FCM-Z4KB). The images derived from the Allen Human Brain Atlas (© 2010 Allen Institute for Brain Science; Allen Human Brain Atlas) can be accessed from: human.brain-map.org. Specific URLs to recreate the following figures are provided: Figure 2b (https://human.brain-map.org/static/brainexplorer), Extended Data Figure 8a (https://human.brain-map.org/microarray/search/show?search_type=user_selections&user_selection_mode=1) and Extended Data Figure 8b (https://human.brain-map.org/microarray/gene/show/605) and source data has been made available. For all clinical measurements and cytokine levels (Extended Data Figure 1-2, Extended Data Figure 6, Extended Data Figure 9d-f), source data has been made available.

Field-specific reporting

Please select the one below that is the best fit for your research. If you are not sure, read the appropriate sections before making your selection.

☒ Life sciences ☐ Behavioural & social sciences ☐ Ecological, evolutionary & environmental sciences

For a reference copy of the document with all sections, see nature.com/documents/nr-reporting-summary-flat.pdf

Life sciences study design

All studies must disclose on these points even when the disclosure is negative.

Sample size	No statistical method was used to predetermine sample size for the analyses (case report, complemented with clinically available samples).
Data exclusions	For clinical and cytokine assays no data points were removed from the analysis. Cytometry data were gated to relevant population as shown in the manuscript. CITE-seq data were filtered to remove multiplets based on the crossSampleDoublets() and withinSampleDoublets() functions of the Citefuse package (v1.2.0) in R (v3.6.1). No other cells were excluded from the analysis.
Replication	As data pertains to a single case report and other patients with similar toxicity profiles were not treated at our site, no additional patients could be assessed. Three additional patients on the same clinical trial and 1 healthy control were used as comparison for the CITE-seq experiment. Public transcriptomic data from 6 healthy donors of the Allen Brain atlas was used to establish RNA expression of the TNFRSF17 (BCMA) gene. Immunohistochemistry successfully confirmed presence of BCMA protein on brain tissue of the patient and 1 control brain.
Randomization	Experiments were not randomized.
Blinding	The investigators were not blinded to allocation during experiments and outcome assessment.

Reporting for specific materials, systems and methods

We require information from authors about some types of materials, experimental systems and methods used in many studies. Here, indicate whether each material, system or method listed is relevant to your study. If you are not sure if a list item applies to your research, read the appropriate section before selecting a response.

Materials & experimental systems

n/a	Involved in the study
☐	☒ Antibodies
☒	☐ Eukaryotic cell lines
☒	☐ Palaeontology and archaeology
☒	☐ Animals and other organisms
☐	☒ Human research participants
☐	☒ Clinical data
☒	☐ Dual use research of concern

Methods

n/a	Involved in the study
☒	☐ ChIP-seq
☐	☒ Flow cytometry
☒	☐ MRI-based neuroimaging

Antibodies

Antibodies used	A full list of antibodies used for mass cytometry, flow cytometry and CITE-seq including vendor and catalog number is available as Supplementary Data. Additional details including dilution are included in the Methods.
Validation	All of the antibodies used in this study were validated for the use in human specimens by the manufacturers and are quality control tested by surface or intracellular immunofluorescent staining with flow cytometry analysis. For more details including full validation information we refer to the manufacturer's website (fluidigm.com, biolegend.com, bdbiosciences.com, thermofisher.com, southernbiotech.com, miltenyibiotec.com)

Human research participants

Policy information about studies involving human research participants

Population characteristics	The CARTITUDE-1 trial (https://clinicaltrials.gov/ct2/show/NCT03548207) is an open-label, single-arm phase 1b/2 trial that

Population characteristics	evaluates safety and efficacy of JNJ-68284528 (ciltacabtagene autoleucel, cilta-cel), a CAR-T cell therapy directed against BCMA in participants with relapsed or refractory MM. Here, we provide the case report of a patient with neurotoxicity enrolled on the CARTITUDE-1 trial. Analysis and reporting follow the CARE guidelines. The CITE-seq experiment includes data on three additional MM patients enrolled on the CARTITUDE-1 trial (61-year-old female, 67-year-old male, 67-year-old female). Furthermore, all MM patients included in this work consented to participation in the Multiple Myeloma Biorepository (HSM:18-00456). All subjects provided written informed consent for the evaluations. All study protocols were approved by the Program for the Protection of Human Subjects (PPHS) and the Institutional Review Board (IRB) at the Icahn School of Medicine at Mount Sinai and adhere to the 2008 Declaration of Helsinki.
Recruitment	The CARTITUDE-1 trial is a multi-center trial with 21 study locations. Patient provided written informed consent for all study protocols involved. The patient in this case report was selected based on the development of a specific adverse event. Three other patients from the same trial used as controls in some experiments were selected based on availability of samples and similarage.
Ethics oversight	All study protocols were approved by the Program for the Protection of Human Subjects (PPHS) and the Institutional Review Board (IRB) at the Icahn School of Medicine at Mount Sinai.

Note that full information on the approval of the study protocol must also be provided in the manuscript.

Clinical data

Policy information about clinical studies

All manuscripts should comply with the ICMJE guidelines for publication of clinical research and a completed CONSORT checklist must be included with all submissions.

Clinical trial registration	A Phase 1b-2, Open-Label Study of JNJ-68284528, A Chimeric Antigen Receptor T-Cell (CAR-T) Therapy Directed Against BCMA in Subjects With Relapsed or Refractory Multiple Myeloma (NCT03548207)
Study protocol	A study description is provided at: https://clinicaltrials.gov/ct2/show/NCT03548207. The report has been published Lancet (Berdeja et al. 2021)
Data collection	The CARTITIUDE-1 trial is active, but not recruiting. Estimated study completion date is April 30, 2022.
Outcomes	Primary outcome in the Phase 1b includes number of participants with adverse events and adverse event severity. An assessment of severity grade will be made according to the National Cancer Institute Common Terminology Criteria for Adverse Events (NCI CTCAE), with the exception of cytokine release syndrome (CRS), and immune effector cell-associated neurotoxicity syndrome (ICANS). CRS and ICANS should be evaluated according to the American Society for Transplantation and Cellular Therapy (ASTCT) consensus grading. Primary outcome in the Phase 2 is overall response rate. The ORR is defined as the proportion of participants who achieve partial response (PR) or better according to International Myeloma Working Group (IMWG) criteria as assessed by the Independent Review Committee (IRC). A full list of predefined secondary outcome measures in this trial can be found online (https://clinicaltrials.gov/ct2/show/NCT03548207).

Flow Cytometry

Plots

Confirm that:

☒ The axis labels state the marker and fluorochrome used (e.g. CD4-FITC).

☒ The axis scales are clearly visible. Include numbers along axes only for bottom left plot of group (a 'group' is an analysis of identical markers).

☒ All plots are contour plots with outliers or pseudocolor plots.

☒ A numerical value for number of cells or percentage (with statistics) is provided.

Methodology

Sample preparation	Cryopreserved Ficoll density separated peripheral blood mononuclear cells were thawed by standard technique. Cells in the CSF were used within 3 hours of collection after isolation. For all flow studies conducted in CSF, cells were obtained by centrifuging and removing supernatant. Cells were washed and stained with antibody cocktail.
Instrument	Samples were acquired on a BD FACS LSR Fortessa Cell analyzer (BD Biosciences)
Software	Events were aquired using BD FACS Diva Software (release 2019). Data was visualized and analyzed using Cytobank software.
Cell population abundance	No sorting experiments were conducted. FACs calibration was done with BD FACSDiva CS&T Research Beads (CAT#655050). UltraComp eBeads (ThermoFisher, CAT#01-2222-42) were used for compensation. Due to the limited cell numbers the entirety of the sample was acquired at once for each sample.

Gating strategy	Gating strategies are shown in the Extended Data. Briefly, for cytometry, lymphocytes were gated using the standard FSC/SSC gating, followed by singlet discrimination. For mass cytometry, DNA stain and viability stain were used to gate intact/live cells respectively. Subsequently, CD45+ CD66b- was used to remove granulocytes and other non-immune cell types. All subsequent manual gating was done with markers optimized to have clear distinction between positive and negative populations.

☒ Tick this box to confirm that a figure exemplifying the gating strategy is provided in the Supplementary Information.